

Journal of Zhejiang University-SCIENCE A (Applied Physics & Engineering)
 ISSN 1673-565X (Print); ISSN 1862-1775 (Online)
 www.jzus.zju.edu.cn; www.springerlink.com
 E-mail: jzus@zju.edu.cn



Review:

Internal flow structure, fault detection, and performance optimization of centrifugal pumps*

Zhe-ming TONG^{1,2}, Jia-ge XIN², Shui-guang TONG^{†‡1,2}, Zhong-qin YANG², Jian-yun ZHAO³, Jun-hua MAO⁴

¹State Key Laboratory of Fluid Power and Mechatronic Systems, Zhejiang University, Hangzhou 310027, China

²School of Mechanical Engineering, Zhejiang University, Hangzhou 310027, China

³Hangzhou Boiler Group Co., Ltd., Hangzhou 310021, China

⁴Wuxi Huaguang Boiler Co., Ltd., Wuxi 214028, China

[†]E-mail: cetongsg@zju.edu.cn

Received Nov. 29, 2019; Revision accepted Dec. 28, 2019; Crosschecked Jan. 7, 2020

Abstract: This review mainly summarizes the latest developments in the internal flow field and external characteristics of centrifugal pumps. In particular, the latest findings of centrifugal pumps focused on turbulence and cavitation models, flow visualization methods, and fault detection based on noise and vibration. The external characteristics, cavitation, and vibration of the centrifugal pump were extensively discussed. In addition, advanced multi-objective optimization methods for improving impeller's efficiency and reducing net positive suction head (NPSH) were briefed. Although some progress was made in this field, there remain many unsolved problems, such as monitoring and modeling of cavitation, rotational stall phenomenon, and discrepancies between simulation and measurement. In the future, researchers are encouraged to employ multi-dimensional flow visualization technologies and high-performance computing facilities to advance existing understandings on these issues and create new research directions.

Key words: Centrifugal pump; Two-phase flow; Cavitation; Pressure pulsation; Multi-objective optimization
<https://doi.org/10.1631/jzus.A1900608>

CLC number: TH311

1 Introduction

Centrifugal pumps are essential mechanical equipment for energy conversion and fluid transportation. They are widely used in agricultural water conservancy construction, petrochemical, electric power, transportation, and metallurgical industries.

Centrifugal pumps consume about 20% of the world's electricity (Mandhare et al., 2019). As one of the world's main sources of power consumption, improving their efficiency and reducing noise and vibration can not only benefit the operation safety and reliability, but also reduce energy cost.

At present, scholars have carried out research on centrifugal pump component design (Bowade and Parashar, 2015; Zhang QH et al., 2019), numerical simulations (Shah et al., 2013), and equipment fault detection (Si et al., 2019). However, issues with regard to the internal and external characteristics, fault detection, and performance optimization were not fully addressed. This paper made an in-depth review on internal flow structure and external characteristics of centrifugal pumps. In addition to a large body of research on improving the energy efficiency of pump

[‡] Corresponding author

* Project supported by the National Key R&D Program of China (No. 2019YFB2004604), the National Natural Science Foundation of China (No. 51821093), the Zhejiang Provincial Natural Science Foundation of China (No. LR19E050002), the Key R&D Program of Zhejiang Province (Nos. 2018C01020 and 2018C01060), and the Youth Funds of the State Key Laboratory of Fluid Power and Mechatronic Systems (No. SKLoFP_QN_1804), China

ORCID: Zhe-ming TONG, <https://orcid.org/0000-0003-1129-7439>

© Zhejiang University and Springer-Verlag GmbH Germany, part of Springer Nature 2020

systems, investigation on vibration monitoring and performance optimization is needed.

This paper first reviews the internal flow structure of the centrifugal pump, which allows us to understand fully the complex flow field and the energy loss mechanism inside the centrifugal pump. Next, a review of the study of the external characteristics of centrifugal pump is presented. Third, the latest research progress in vibration monitoring and fault detection of centrifugal pump is introduced. Finally, various methods and measures for optimizing the performance of the centrifugal pump are described.

2 Internal flow structure of centrifugal pump

2.1 Computational fluid dynamics model of centrifugal pump

2.1.1 Turbulence model

The complex shape and structure of the centrifugal pump make it necessary to consider several geometric parameters in the design of the centrifugal pump, which is also a great challenge to the performance prediction of the centrifugal pump (Jafarzadeh et al., 2011). Computational fluid dynamics (CFD) methods are used to test the performance of a computational prototype, which can well predict the performance of fluid machinery at the drawing design stage. Numerical simulation provides a wealth of flow field information, providing a basis for engineers to design and improve fluid machinery. Therefore, many centrifugal pump researchers have used CFD for the fluid dynamic design of pumps.

Solving the continuous equation and the Reynolds average Navier-Stokes (RANS) equation, and then closing the equation with a turbulence model, has gradually become the main method for numerical calculation of centrifugal pumps. The commonly used RANS turbulence models for centrifugal pump CFD calculations include: the $k-\varepsilon$ model, the renormalization group (RNG) $k-\varepsilon$ model, and the shear stress transfer (SST) $k-\omega$ model. The $k-\varepsilon$ model is currently the most widely used of the engineering turbulence models (Tan et al., 2015). The equation uses the deceptive scale as the feature length and is obtained by solving the corresponding partial differential equation. Studies have shown that it performs better flow field predictions for the complex 3D turbulence of centrifugal pumps. The $k-\varepsilon$ model has proven to be a

good method for studying the flow dynamics of the near-lobe region of a leafless centrifugal pump (Barrio et al., 2010).

The RNG $k-\varepsilon$ model has great advantages in predicting turbulence caused by shearing motion (Guleren and Pinarbasi, 2004; Derakhshan et al., 2013). The SST $k-\omega$ model has important improvements in the prediction of backpressure gradient flow (Shojaeefard et al., 2012). The near-wall flow can be evaluated with high precision using the $k-\omega$ model and the SST function (Pei et al., 2013). The SST $k-\omega$ model has been used to study flow in impellers and diffusers to accurately predict the hydraulic head and flow structure of the pump (Zhou et al., 2015). Selecting different RANS turbulence models is slightly different from the calculation results, and it is necessary to compare and select the appropriate model according to the actual situation.

The RANS model indicated to be unsuitable for the calculation of transient turbulent separation flows in centrifugal pumps (Byskov et al., 2003; Benim et al., 2008). Simulation strategies such as direct numerical simulation (DNS) and large eddy simulation (LES) are potential alternatives to flow field prediction in RANS (Jafarzadeh et al., 2011). However, they have a higher computational cost in solving boundary layer turbulence at higher Reynolds numbers.

Byskov et al. (2003) compared the LES simulation results of the centrifugal pump under steady-state operation with the RANS numerical results and performed verification evaluation by particle image velocimetry (PIV) measurement. The predicted velocity from LES was compared with experimental data to confirm the existence of a combination of non-rotating stall and relative eddy current. However, RANS had a lower accuracy in predicting complex flows in the flow field.

The LES method is based on a second-order exact numerical method combined with a vortex viscosity subgrid-scale (SGS) model to simulate turbulence, and Yang et al. (2012) evaluated the Smagorinsky model (SM), dynamic Smagorinsky model (DSM), and dynamic mixed model (DMM). The simulation results showed that the DMM model could accurately capture the turbulent structure details of the large curvature flow field of the centrifugal pump.

Studies of turbulence models of centrifugal pumps are summarized in Table 1. Using CFD to

Table 1 Summary of turbulent model of centrifugal pump

Reference	Turbulence model	Test case or test region
Guleren and Pinarbasi, 2004	$k-\varepsilon$	Studied the effects of blade number and the relative position between blade and volute tongue on centrifugal pump based on RNG $k-\varepsilon$ turbulence model
Zhang N et al., 2016	LES	Analyzed unsteady rotor-stator interaction and flow structures within a low specific-speed centrifugal pump using LES method
Posa et al., 2011	LES	Reported one of the first LES in turbulent and transitional flows
Barrio et al., 2010	URANS+ $k-\varepsilon$	Simulated the unsteady flow field by the CFD program to study the dynamic characteristics of the flow near the tongue of the vane centrifugal pump
Pei et al., 2013	URANS+SST $k-\omega$	Carried out a CFD simulation and new flow unsteadiness analysis for a single-blade centrifugal pump with whole flow passage
Jafarzadeh et al., 2011	$k-\varepsilon$, RNG $k-\varepsilon$, RSM	Presented a general 3D simulation of the turbulent fluid flow to predict the velocity and pressure fields for a centrifugal pump and analyzed the effect of blade number of the characteristics of the pump
Kaewnai et al., 2009	$k-\varepsilon$, $k-\omega$, RNG $k-\varepsilon$	Used CFD technique to analyze and predict the performance of a radial flow-type impeller of a centrifugal pump
Yang et al., 2012	LES	Studied three SGS models including SM, DSM, and DMM using CFD code FLUENT combined with its user defined function
Tan et al., 2015	RNG $k-\varepsilon$	Revealed and analyzed the detailed flow field and cavitation effect on partial load
Derakhshan et al., 2013	RNG $k-\varepsilon$	Proposed an optimal design method of impellers based on ANS and ABC algorithm, and verified it by CFD method
Shojaeefard et al., 2012	SST $k-\omega$	Numerically simulated the 3D flow in centrifugal pump that pumps viscous fluid along with the volute
Zhou et al., 2015	SST $k-\omega$	Compared CFD investigation and PIV validation of flow field in a compact return diffuser under strong part-load conditions
Byskov et al., 2003	LES	Investigated the flow field in a shrouded six-bladed centrifugal pump impeller at design load and quarter-load using LES

URANS: unsteady Reynolds average Navier-Stokes; RSM: Reynolds stress model; ANS: artificial neural networks; ABC: artificial bee colony

simulate and predict unsteady flow in centrifugal pump is of great significance for improving performance. The use of more advanced turbulence models to capture complex flow characteristics will help to improve and optimize the centrifugal pump design and achieve an accurate prediction of centrifugal pump performance.

2.1.2 Cavitation model

At present, the numerical simulation of the centrifugal pump cavitation problem primarily uses the cavitation model (Bilus and Predin, 2009; Ding et al., 2011; Wang Y et al., 2016; Hu et al., 2019). The choice of cavitation models is critical to the accurate prediction of cavitation flow.

(1) The full cavitation model (Singhal et al., 2002) considers phase change, bubble dynamics, turbulent pressure fluctuation, and non-condensable

gases. It has higher prediction accuracy for the critical cavitation value of the centrifugal pump and has better consistency with the experimental values (Ding et al., 2011). The full cavitation model and the RNG $k-\varepsilon$ turbulence model were used to simulate and compare the gas volume fraction in the impeller under partial flow conditions. However, the capture of the cavitation separation state is rather blurred (Tan et al., 2012, 2013). The full cavitation model can provide a wide range of cavitation domains, but the capture of bubble morphology is not obvious enough, the calculation is difficult, and the convergence is poor.

(2) The Zwart-Gerber-Belamri model assumes that all bubbles are about the same size, and the number of bubble densities of the interphase mass transfer rate is determined, while ignoring the bubble surface tension and the second derivative term. The Zwart-Gerber-Belamri cavitation model is used to

predict the development of cavitation in the entire impeller channel. The predicted trend is qualitatively and quantitatively consistent with the experimental results (Meng et al., 2016). However, this model ignores the influence of non-condensing gases, resulting in greater empirical constants in the formula. If these empirical constants are chosen improperly, it may have a greater impact on the results.

(3) The formula of the traditional turbulence model is derived from the non-cavitation flow, so the application of the eddy viscosity model in complex turbulent cavitation flow is greatly limited (Liu et al., 2009; Bensow and Bark, 2010; Lu et al., 2010). For many years, researchers have been working to correct turbulence in cavitation simulations by modifying turbulent viscosity (Tan et al., 2012).

In recent years, a filter-based model (FBM) combining the standard $k-\varepsilon$ model with LES has been gradually applied to the simulation of turbulent cavitation flow in centrifugal pumps (Chen et al., 2017a; Lin and Xue, 2018). By comparing the application of RANS and FBM methods in cavitation flow of centrifugal pump impeller, it was determined that FBM is helpful for reducing the dependence of the traditional vortex viscosity model and turbulence amount on inlet vortex viscosity, and its prediction accuracy is higher, which is more consistent with experimental visualization than other results (Liu et al., 2013a).

A newly developed cavitation flow calculation model is proposed, which is a two-phase, three-component calculation model (Wang Y et al., 2016). Improving the FBM model based on the RNG $k-\varepsilon$ model was achieved by using probability density functions. Also considered was the impact of pressure fluctuations on turbulence to modify the Kunz cavitation model. The modified Kunz model was used as the cavitation model, and the modified FBM model was used as the turbulence model. Three numerical schemes were considered for comparison (Table 2), which showed the vapor volume fraction distribution on the suction side of the blade inlet edge with a flow coefficient ψ of 0.114 for three numerical simulations

and the experimental test (Fig. 1). The bubble distribution shows that schemes 2 and 3 were more accurate in prediction. Throughout the article (Wang Y et al., 2016), scheme 3 better predicted critical cavitation numbers of a centrifugal pump as compared to scheme 2.

(4) The thermodynamic effect is an important factor in the vapor-liquid conversion of cavitation flow, but the above cavitation models were not considered. A cavitation model that considers mass, momentum, and energy transportation is developed on the basis of the Rayleigh-Plesset dynamic equation for bubbles and the Plesset-Zwick equation for cavitating thermodynamic mechanisms (Tang et al., 2013).

The proposed cavitation model was used to simulate the centrifugal pump and compared with the simulation results of the full cavitation model. As can be seen from Fig. 2, the performance curve calculated by using the proposed cavitation model drops more steeply, due to the bubble burst from the inlet to the outlet of the impeller, causing the release of heat and the temperature of the flow field to rise, and thus exacerbating the deterioration of performance (Tang et al., 2013). Hu et al. (2019) explored the law of cavitation jet cleaning technology in underwater jet flow through CFD simulation and obtained accurate results. Therefore, the proposed cavitation model considering thermodynamic effects should be considered in engineering.

The current cavitation model is based on different assumptions about bubbles and more or less omitted from real physical properties. For centrifugal

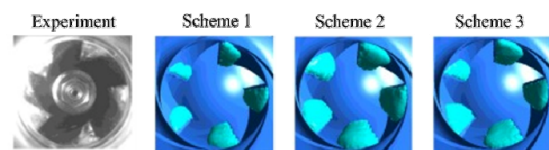


Fig. 1 Vapor volume fraction distribution in the suction side of the blade inlet edge when the flow coefficient ψ is 0.114

Reprinted from (Wang Y et al., 2016), Copyright 2016, with permission from Elsevier

Table 2 Three numerical schemes in (Wang Y et al., 2016)

Scheme	Turbulence model	Cavitation mode	Incompressible gas
1	RNG $k-\varepsilon$ model	Zwart model	Not considered
2	FBM filter model based on RNG $k-\varepsilon$ model	Kunz model	Not considered
3	Modified FBM filter model based on RNG $k-\varepsilon$ model	Modified Kunz model	Considered

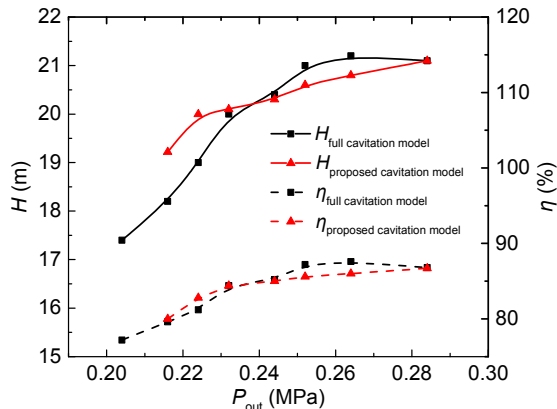


Fig. 2 Predicted cavitation performance

H is the head; P_{out} is the outlet pressure; η is the efficiency. Reprinted from (Tang et al., 2013), Copyright 2013, with permission from Springer Science+Business Media

pump flow fields with complex turbulence and cavitation, the more adaptable model should be considered according to the specific situation.

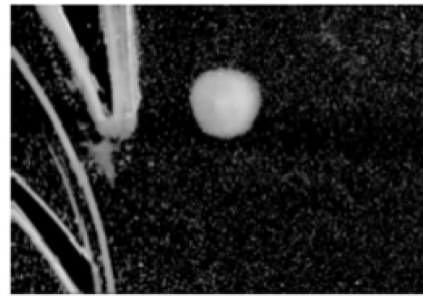
2.2 Visualization method for internal flow of centrifugal pump

Experimental testing is the most basic and credible method for understanding various methods of internal flow field in centrifugal pumps (Liu et al., 2013c). However, the special geometry of the centrifugal pump and the complex internal flow impose very stringent requirements on the experimental measurement technique. The development of mobile display technology is being increasingly perfected. Laser Doppler velocity (LDV) technology and PIV techniques are widely used for the observation of centrifugal pump flow structures. Because optical technology is not invasive, it does not cause external interference in the flow field (Wu et al., 2011).

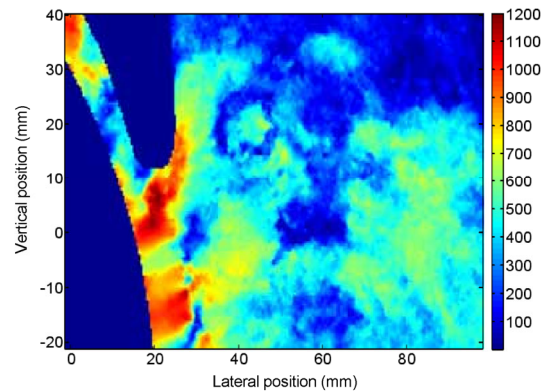
Scholars have used LDV to measure many flow fields. LDV measured the velocity field of multiple complex flows inside the impeller, demonstrating the effect of hydraulic loss on flow (Miner et al., 1989). LDV was used to study the unsteady complex flow structure at the exit portion of the impeller (Li, 2008; Feng et al., 2011). LDV provides accurate flow field results as measurements are made directly at the point of interest.

PIV technology is a powerful alternative or complement to LDV, which provides more information about the instantaneous spatial flow structure while greatly reducing acquisition time (Pedersen et

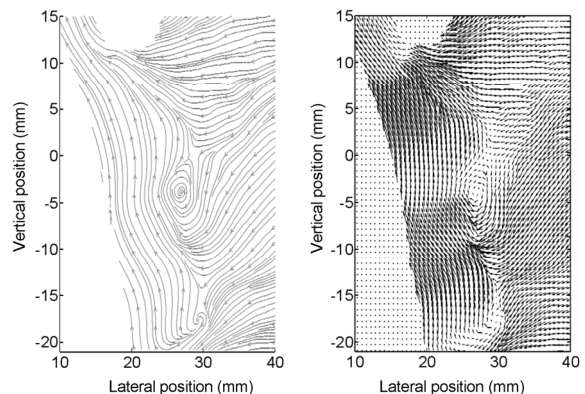
al., 2003). Fig. 3a is the original image of the centrifugal pump tongue captured by PIV, and Figs. 3b–3d are the velocity cloud map, flow field streamline map, and flow field velocity vector diagram obtained after the original image is subjected to flow field post-processing. PIV can clearly identify the vortex structure inside the flow field, which can best describe the average relative and absolute velocities of the phases in the plane, the turbulence energy, and the



(a)



(b)



(c)

(d)

Fig. 3 Flow at the volute of a centrifugal pump taken with PIV (Huang, 2019)

(a) Original image; (b) Velocity map; (c) Flow field streamline diagram; (d) Flow field speed vector

calculation of the vortex field (Fig. 4). It also perfectly captures the evolution of the phase over time in a blade channel.

PIV was widely used in the observation and measurement of centrifugal pumps, such as the velocity distribution at the interference between the volute tongue and the impeller (Shao et al., 2015), kinetic energy fluctuations (Kadambi et al., 2004), the entire flow field inside the guide vane and diffuser channel (Gaetani et al., 2012; Keller et al., 2014), vorticity distribution in pumps (Zhang et al., 2018), and unsteady flow characteristics of pumps (Liu et al., 2013c; Keller et al., 2014; Si et al., 2015). PIV measurements can also be used to verify the results of CFD (Feng et al., 2007, 2009).

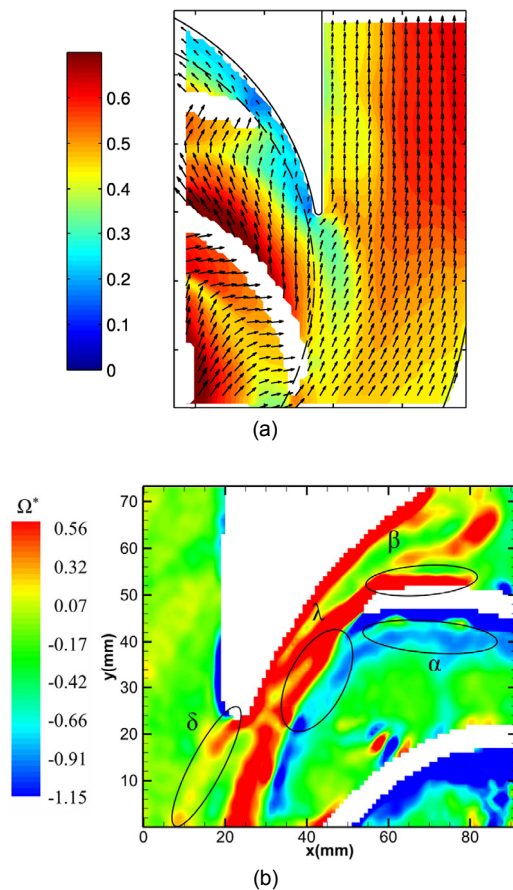


Fig. 4 Normalized phase average of the tongue region taken using PIV

(a) Velocity distribution; Reprinted from (Keller et al., 2014), Copyright 2014, with permission from Springer Science+Business Media. (b) Vorticity distribution; Reprinted from (Zhang et al., 2018), Copyright 2018, with permission from Elsevier

2.3 Internal flow phenomenon

2.3.1 Unsteady flow features

The coupling between rotor and stator, blade and fluid determines that the centrifugal pump has the first kind of unsteady flow, that is, the response of viscous flow under external disturbance (Shao et al., 2015; Cheng et al., 2019). Secondly, the viscous fluid forms a boundary layer at the solid boundary of the runner. Under the action of centrifugal force and Coriolis force, the boundary layer forms different degrees of separation. The unsteady flow caused by the flow itself is the second kind of unsteady flow inside the centrifugal pump (Si et al., 2015). In addition, for multistage centrifugal pumps, the wake of the upper stage passes through the gapless gap and then enters the next stage, resulting in a more complex unsteady flow in the next stage. The existence of complex unsteady flows at the next level will inevitably affect the flow of the upper level (Stel et al., 2013).

Studies have shown that under different operating conditions, there is flow separation inside the centrifugal pump (Zhang et al., 2018), secondary flow (Westra et al., 2010), gap flow (Ayad et al., 2015), multiphase flow (Bachert et al., 2010), and other complex flow phenomena.

2.3.2 Flow field during transient operation

Typically, the pump has transient operation, such as pump start and stop, increased and decreased flow, and power failure of the centrifugal pump motor (Wu et al., 2010). In these operations, the response of the pump system can have a transient effect due to changes in operating conditions.

During pump start-up, the pump speed increases rapidly from zero to thousands of revolutions. The characteristic Reynolds number increases rapidly from zero to millions, and the internal turbulent state changes from laminar flow to high turbulence, including dynamic and static interference between the blade and the tongue. The start-up process of the centrifugal pump is related to the acceleration of the start-up and is also related to the speed at which the start-up is completed, the resistance of the pipeline, and the shape of the pump (Chalghoum et al., 2016). The internal influencing factors are fluid viscosity, inertia, and changes in instantaneous flow regimes,

such as changes in flow parameters and development of vortices in the flow field (Zhang YL et al., 2016).

Li et al. (2010) proposed a dynamic slip region method for transient flow evolution during the simulation start-up process. Fig. 5 is the transient simulation of the impeller inlet when the centrifugal pump is started. At the beginning of the start-up, a large vortex is visible at the impeller inlet. This compact vortex that occurs during transient start-up is the direct cause of the lower transient head (Li et al., 2011).

At present, most of the internal transient flow research on the start-up process of the centrifugal pump is carried out. However, the transient inflow evolution mechanism during cavitation in the start-up process, the transient performance of the centrifugal pump during shutdown, and the pressure pulsation of the pipeline resistance transient process still need to be explored further.

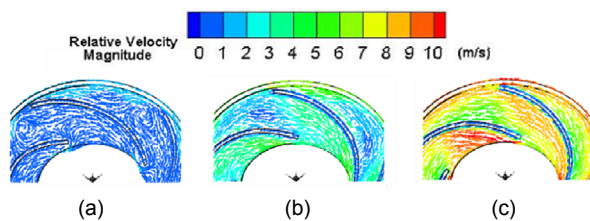


Fig. 5 Instantaneous relative velocity evolution at the impeller inlet (reference frame is fixed on the impeller, $0.1 \text{ s} \leq t \leq 1.6 \text{ s}$)

(a) Time $t=0.1 \text{ s}$; (b) $t=0.5 \text{ s}$; (c) $t=1.6 \text{ s}$. Reprinted from (Li et al., 2011), Copyright 2011, with permission from Springer Science+Business Media

2.4 Research status on gas-liquid two-phase flow

Centrifugal pump has indispensable application value in the petroleum industry (Scott, 2003; Caridad et al., 2008). However, if the pressure inside the pump is lower than the saturated oil pressure during operation, gas will be produced, forming a mixture of gas and liquid (Monte Verde et al., 2017). As the gas volume fraction (GVF) continues to increase, the flow pattern in the impeller changes, directly leading to a decrease and deterioration of pump performance. The change of the flow field and performance caused by gas-liquid two-phase flow of centrifugal pump is the main focus of current research.

Visualization techniques can obtain quantitative information about variables in the flow field, such as

bubble size distribution and velocity. Most laboratories do not allow testing of oil and gas mixtures for safety reasons (Zhang JY et al., 2016; Monte Verde et al., 2017; Shao et al., 2018; Tong ZM et al., 2019c). Therefore, a mixture of water and air was selected for experimental study. The results obtained are helpful for scholars to better understand the phenomenon and rule of gas-liquid two-phase flow in centrifugal pump. In addition, these results can be used as a reference for numerical simulation verification.

The fluid property, flow rate, and impeller shape mainly determine the change of flow pattern caused by the interaction of gas-liquid two phases (Zhu and Zhang, 2018). In the latest research, high-speed photography was used to study the flow patterns and characteristics of the pump (Monte Verde et al., 2017). With the increase in GVF, four types of flow patterns were captured and identified. The identification of the four flow patterns is well matched to various previous studies on flow patterns (Murakami and Minemura, 1974a, 1974b; Sato et al., 1996; Scott, 2003; Schäfer et al., 2015; Mansour et al., 2018).

When the local GVF inside the vane passage is low (from 0% to 4%), there is a uniform flow bubble flow state (Fig. 6a). The phase slip causes the bubbles to agglomerate (Jiang et al., 2019), forming agglomerated bubble streams (Fig. 6b). The dispersed bubbles continue to evolve toward the slug flow and form a gas-pocket flow (Fig. 6c) with an increased bubble size (Sekoguchi et al., 1984). The bubbles collect on the pressure side of the impeller blades and occupy a large portion of the impeller passage, resulting in the extremely limited available area for liquid flow (Poullikkas, 2003; Barrios and Prado, 2011). As the GVF increases, the gas-pocket flow becomes a separate flow (Fig. 6d), and small bubble flow and fixed large bubbles occur simultaneously (Sato et al., 1996), while the pump head is significantly reduced (Schäfer et al., 2015). The bubbles increase hydraulic losses and reduce the ability of the impeller to change the momentum of the mixture. As a result, the head delivered by the pump is reduced (Caridad et al., 2008).

Monte Verde et al. (2017) correlated the topological distribution of each stage of the gas-liquid flow mode of the centrifugal pump impeller. Under the condition of a certain speed and inlet pressure, the performance of the pump when the mass flow rate of

the gas is changed is shown in Fig. 7. The changes of flow patterns were observed under the above conditions, and the distributions of the four flow patterns were divided in Fig. 7. The dashed line represents the boundary between the flow states. The pump performance curves are similar under different gas mass flow rates, and all begin to deteriorate with the appearance of gas-pocket flow patterns. The presence of segregated flow may cause the inability of the pump to generate pressure and cause serious damage.

If the gas volume fraction exceeds a certain value, the pump will reach a state called an air lock, in which case the pump will be blocked by the gas and stop working (Zhang JY et al., 2016). Currently, most articles only consider low GVF (<10%), but industrial applications have exceeded this value (Caridad et al., 2008), and there are few studies on extending the range of the GVF value. The experimental data on which most of the gas-liquid two-phase flow pattern diagrams in centrifugal pumps are based are from water-air flow, so the applicable scope of flow pattern diagrams is also limited.

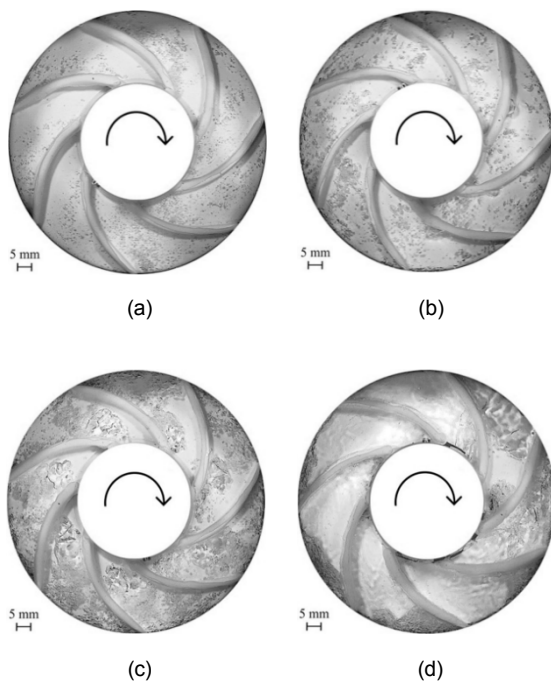


Fig. 6 Four types of flow patterns

(a) Bubble flow pattern; (b) Agglomerated bubble flow pattern; (c) Gas-pocket flow pattern; (d) Segregated flow pattern. Reprinted from (Monte Verde et al., 2017), Copyright 2017, with permission from Elsevier

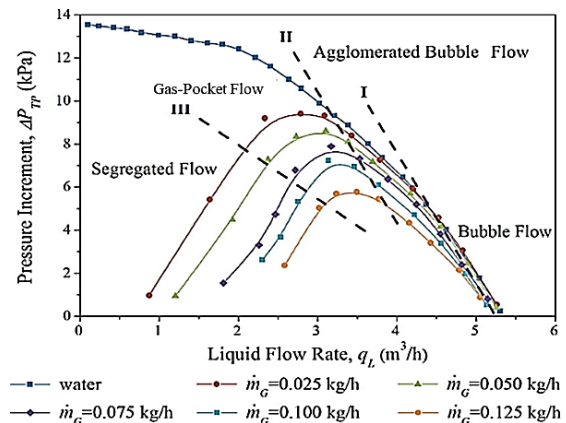


Fig. 7 Relationship between the flow patterns and pump performance under different gas mass flow rates, \dot{m}_g

Reprinted from (Monte Verde et al., 2017), Copyright 2017, with permission from Elsevier

2.5 Cavitation flow mechanism

Cavitation is the compressible and unsteady turbulent flow caused by the mass transfer between gas and liquid phases (Wang et al., 2001). The effects of cavitation on hydrodynamics are usually noise (Chudina, 2003), vibration (Benaouicha et al., 2010; Wang et al., 2015), material damage (Mouvanal et al., 2018), and performance degradation (Tao et al., 2018a). The guarantee of cavitation performance is often very important when designing a centrifugal pump (Hirschi et al., 1998).

The leading edge of the centrifugal pump blade is the place where the pressure is the least and cavitation occurs first (Tan et al., 2014b). Figs. 8a–8d show the numerical results of the cavitation deterioration process of the centrifugal pump when the total inlet pressure drops below the vapor pressure at a low flow rate (79% of the optimal flow rate Q_0). At low flow rates, the typical development of cavitation is asymmetric (Fu et al., 2015; Tao et al., 2018a). As the total inlet pressure decreases, adherent cavities of different lengths are formed on adjacent blades (Tao et al., 2018a). The cavity on the blade gradually diffuses to the middle of the blade from the suction surface near the leading edge. In one of the blades, the cavitation reaches its maximum strength and the vapor volume occupies the entire blade.

Figs. 9a–9e show the cavitation structure of centrifugal pump at high flow rate (120% of the optimal flow rate Q_0). Its cavitation structure is completely different from the flow pattern observed

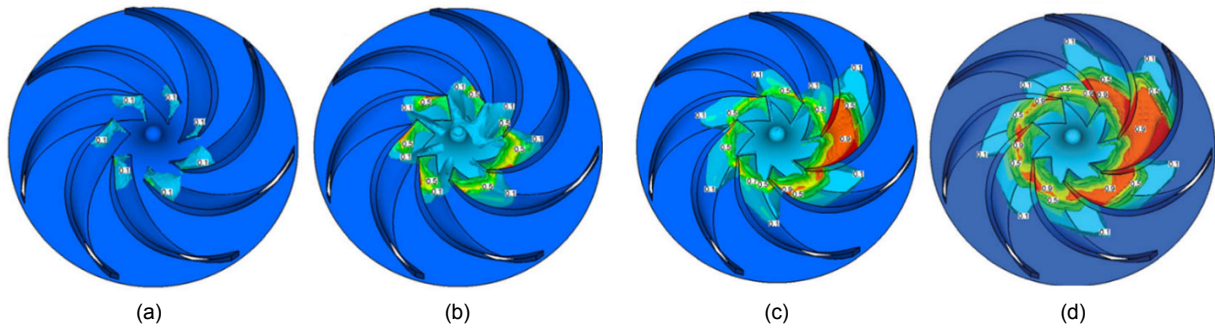


Fig. 8 Vapor structures in the test pump at a low flow rate (79% of the optimal flow rate Q_0) as the inlet total pressure decreases (Tan et al., 2013): (a) $H_{NPSHa}=2.08$ m; (b) $H_{NPSHa}=1.44$ m; (c) $H_{NPSHa}=1.30$ m; (d) $H_{NPSHa}=1.27$ m
 H_{NPSHa} indicates the net positive suction head available

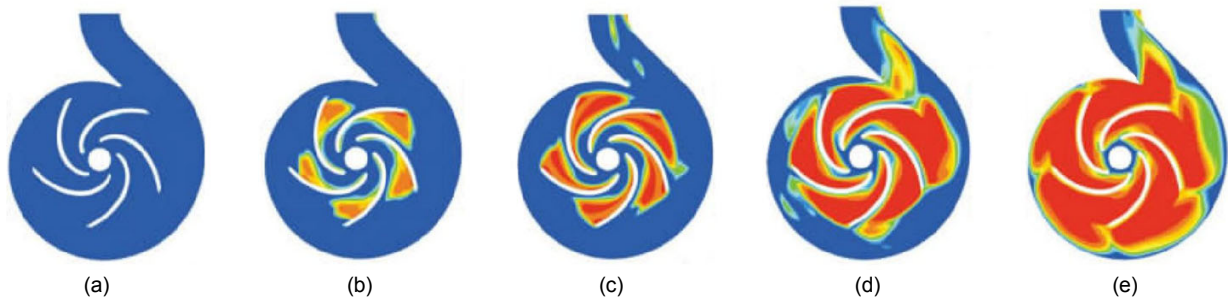


Fig. 9 Vapor structures in the test pump at a high flow rate (120% of the optimal flow rate Q_0) as the inlet total pressure decreases (Wang, 2016): (a) $H_{NPSHa}=4.24$ m; (b) $H_{NPSHa}=3.06$ m; (c) $H_{NPSHa}=2.59$ m; (d) $H_{NPSHa}=1.28$ m; (e) $H_{NPSHa}=1.05$ m

at low flow rates. The cavitation in the impeller develops in a symmetrical manner and, as the inlet pressure decreases, all of the vane passages tend to be evenly filled with vapor (Fu et al., 2015; Meng et al., 2016; Tao et al., 2018a). The suction surface of the impeller is still occupied by most of the cavity. Also, these cavities are formed only inside the pump and do not extend into the inlet pipe.

The main reason for this difference is the large positive attack angle under low discharge condition and the small negative attack angle under high flow condition (Meng et al., 2016). At a low flow rate where no cavitation occurs (Fig. 10a), the positive angle of attack present on the suction side of each blade results in the presence of a vortex. As the net positive suction head (NPSH) decreases (Fig. 10b), a higher reverse pressure gradient causes the vortex to develop toward the leading edge of the blade, and the inlet flow coefficient decreases locally, resulting in a decrease in the cavity of the passage. The pressure distribution during high flow conditions is different from the low flow rate, so the distribution and

development of the cavity are completely different under the two conditions.

Bachert et al. (2010) observed that cavitation at the volute tongue of the pump precedes cavitation on the blade under high flow conditions. This is a special case. The velocity direction at the trailing edge of the blade does deviate from the zero-attack angle of the tongue, and there is a significant oscillation, resulting in cavitation on the tongue. The reverse flow caused by the interaction between the impeller and the tongue is the main cause of unsteady cavitation and pressure fluctuations in the pump (Shi et al., 2014; Meng et al., 2016; Li XJ et al., 2018). Li XJ et al. (2018) found that increasing the radial clearance between the impeller and the volute tongue and changing the edge of the tongue and the trailing edge of the blade is an effective and reasonable way to reduce the pressure pulsation amplitude caused by cavitation. Increasing spiral sub-blades (Chen et al., 2017b) and splitter blades (Yang et al., 2014), appropriate number of induction wheels (Guo et al., 2016), and optimizing blade leading edge shape (Tao et al., 2018a) can

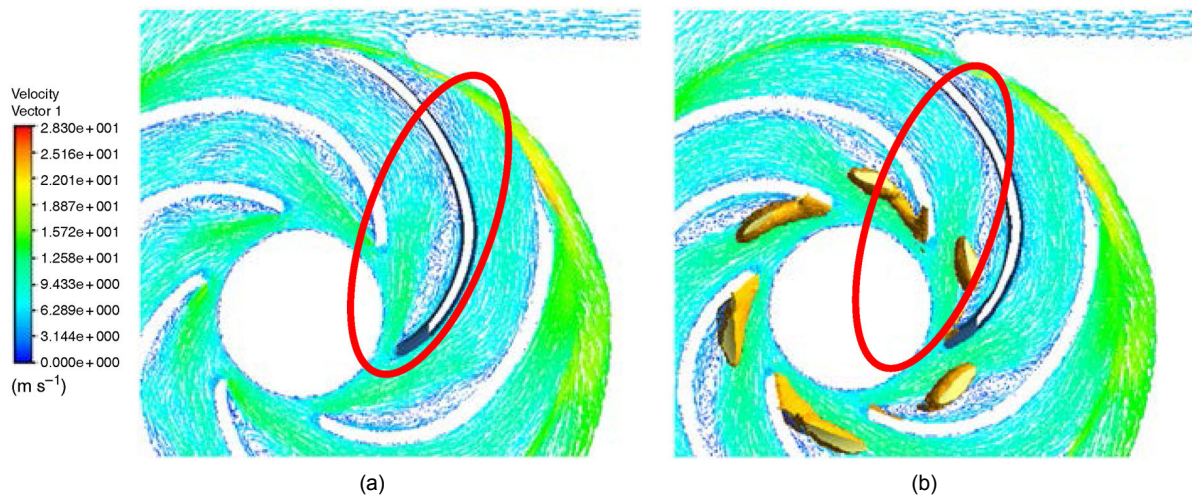


Fig. 10 Velocity distribution in the same blade channel at a low flow rate (70% of the optimal flow rate) (a) No cavitation; (b) Cavitation. Reprinted from (Meng et al., 2016), Copyright 2016, with permission from Emerald Publishing Limited

effectively improve the hydraulic performance and cavitation performance of centrifugal pumps.

3 External characteristics of centrifugal pump

In engineering applications, the main concern is the external characteristics of the centrifugal pump, such as whether the head and flow meet the application standard, whether efficiency is relatively high, how much energy-saving effect is achieved, whether the vibration and noise meet the requirements in the process of operation, and whether the service life is sufficient. The basic parameters characterizing the main performance of the centrifugal pump include flow rate (Q), head (H), power (P), efficiency (η), NPSHr, and speed (n).

3.1 External characteristics under off-design conditions

The centrifugal pump has unstable operation under small flow conditions, and the external characteristic shows a positive slope of the head-flow curve. The internal flow is characterized by unstable phenomena such as stall and separation. The flow in the impeller flow channel is relatively stable and uniform under large flow. Due to the jet-wake effect, the static pressure near the tongue is lower, which

makes the pump more prone to cavitation (Bachert et al., 2010).

Meng et al. (2016) conducted numerical simulation and experimental tests on the cavitation process of centrifugal pumps under low flow, design flow, and high flow rates (46%, 70%, 100%, and 130% of the optimal flow rate Q_0). Fig. 11 shows the head-NPSH and efficiency-NPSH curves at different flow rates. The head reduction rule is similar in different flow rates, as is the efficiency reduction rule. With the decrease of NPSH, the head and efficiency of the pump change little at first. Once the lower NPSH is reached, cavitation failure shows a downward trend in pump head and efficiency. This is consistent with the typical behavior that has been observed in other centrifugal pumps (Medvitz et al., 2002; Tan et al., 2012; Liu et al., 2013b; Wang et al., 2015).

As shown in Fig. 12, the cavity mostly adheres to the suction side during the reduction of NPSHa and gradually blocks the entire blade passage. The vortex in the wake of the cavity is in the middle of the channel, and a high kinetic energy nucleus appears at the trailing edge of the suction blade near the tongue. The impeller cannot convert high kinetic energy into potential energy under vortex flow. Drop of pump head is inevitable (Li et al., 2013).

Under high flow rates, the pump head remains almost constant, and a sudden drop occurs when the critical point is reached (Fu et al., 2015). The critical

NPSH under large flow conditions is higher than those of small flow conditions and design conditions, indicating that the anti-cavitation performance of the centrifugal pump is reduced with increasing flow rate, and the pump is more prone to cavitation. Under the condition of small flow, the drop of the head is slower and slightly rises before the decline. It can be understood that the bubble burst produces a certain pressure wave, and the head rises.

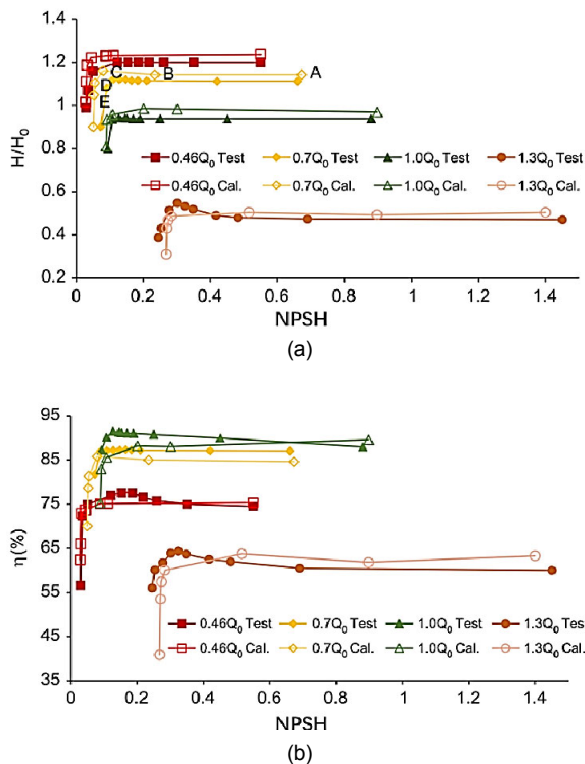


Fig. 11 Head-NPSH curves (a) and efficiency-NPSH curves (b) at different flow rates

Cal. represents calculation result. Reprinted from (Meng et al., 2016), Copyright 2016, with permission from Emerald Publishing Limited

3.2 Effect of speed on the external characteristics

When designing and selecting a centrifugal pump, it is necessary to consider the situation when the centrifugal pump meets the maximum flow and head. Centrifugal pumps with a flow rate and a head that far exceed the actual demand are generally selected. In order to achieve cost-effective operation of the centrifugal pump, reducing the speed is a more effective, convenient, and economical way.

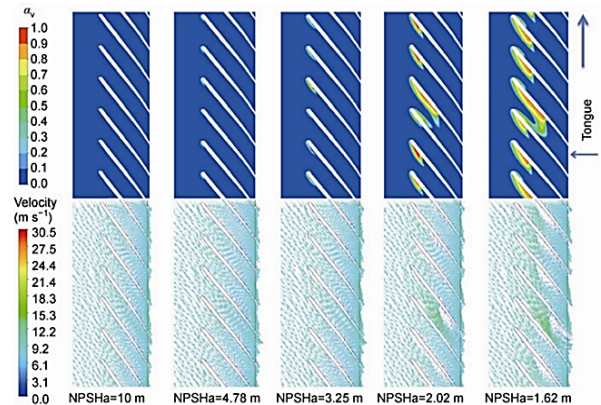


Fig. 12 Vapor volume fraction (α_v) and velocity distribution in blade-to-blade view at 0.7 span

Reprinted from (Li et al., 2013), Copyright 2013, with permission from Springer Science+Business Media

Comparing the $H-Q$ and $\eta-Q$ curves at three speeds, as shown in Fig. 13, it can be seen that as the speed decreases, the head decreases, the efficiency increases, and the flow rate decreases at the highest efficiency point, but the steeper the efficiency curve, the narrower the range of efficient workflows (Zhou et al., 2016). This means that the lower the speed, the narrower the working range of the pump.

Jiang (2015) used the energy gradient method (Dou and Jiang, 2013) to analyze the flow instability at different flow rates inside the centrifugal pump, as shown in Fig. 14. As the rotational speed decreases, the energy gradient function of the internal flow field decreases, making the flow more stable. This is one of the main reasons why efficiency increases with the decrease in rotational speed.

3.3 Hydraulic loss due to overcurrent components

The energy obtained by the effective fluid flowing through the impeller with the rotation of the impeller is not fully converted into the pressure energy of the fluid, because the fluid flowing through the impeller and volute of the pump is accompanied by hydraulic friction loss and hydraulic loss caused by outflow, impact, and changes in speed and direction. Part of the energy is consumed by the shaft rotation.

The energy lost by unit mass fluid flowing through the flow parts of the pump is called hydraulic loss of the pump. Hydraulic loss in centrifugal pump is mainly generated by the impeller, volute, and other over-flow components. Reducing hydraulic loss is the

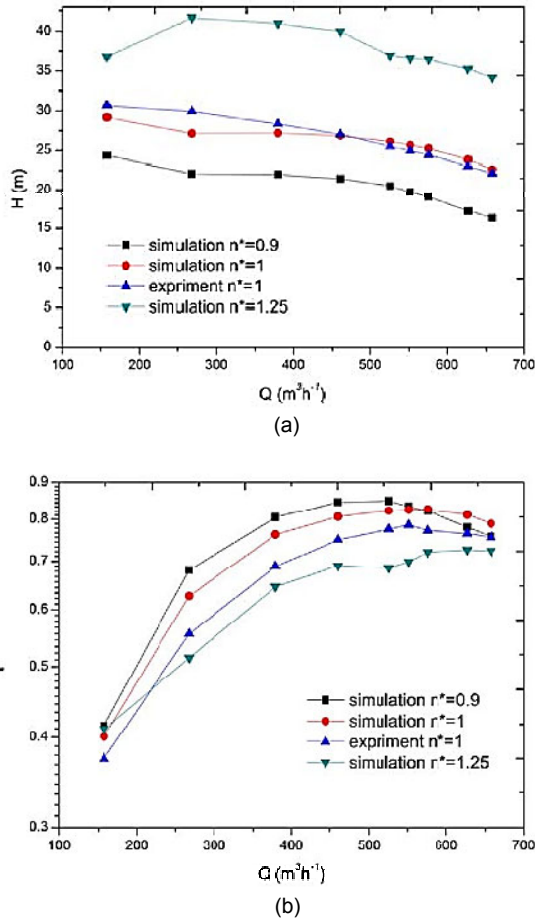


Fig. 13 Pump performance comparisons with different rotating speeds n^* (Jiang, 2015)

(a) $H-Q$ curves; (b) $\eta-Q$ curves

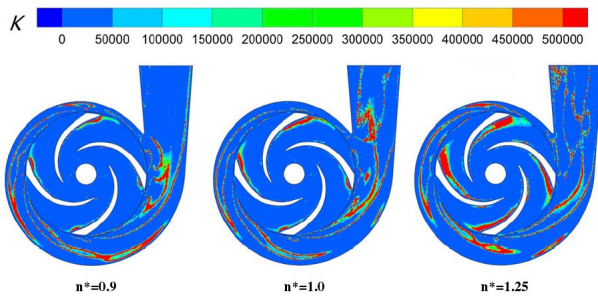


Fig. 14 Distribution of the energy gradient function K of the central plane at different rotational speeds n^* (Jiang, 2015)

main method to improve centrifugal pump efficiency (Wang C et al., 2017). By studying the flow in the volute, it was found that reducing the hydraulic loss

caused by the outlet vortex between the impeller and the volute can effectively improve the performance of the pump (Shojaeefard et al., 2012). Circular section volutes have higher head and efficiency than other sections in almost the entire flow range (Alemi et al., 2015).

Tan et al. (2014b) found that the pre-rotation adjustment of the inlet guide vane (IGV) widened the efficient area under off-design conditions. Pumps using IGV are more efficient than pumps that do not use IGV, and the maximum efficiency is improved by more than 2.0% under design conditions. Due to the change in the peripheral speed at the impeller inlet caused by the IGV, the head is either reduced or increased under positive or negative pre-rotation, respectively. When the IGV is installed, the cavitation performance of the centrifugal pump is reduced, but the change in NPSH is less than 0.5 m.

4 Fault detection based on noise and vibration

Long-term operation in the vibration state will damage the inner surface of the liquid-carrying component, resulting in wear and material removal, which leads to damage and premature failure of hydraulic and machine components, such as impeller blades, shafts bearings, and mechanical sealing surfaces (Wood et al., 1960; Brennen, 2005; de Giorgi et al., 2015). The vibration and noise signals contain a wealth of operating information, and are easy to collect. They can be applied to fault detection of centrifugal pumps. Therefore, using modern signal processing technology to explore the fault feature extraction and pattern recognition of centrifugal pumps is an important research direction at present.

4.1 Noise and vibration

Many scholars have found a close relationship between vibration and cavitation of centrifugal pumps. Zargar (2014) used a condition monitoring system to detect cavitation in the pump and analyzed the vibration signal in both time and frequency domains, finding that the vibration signal suddenly increased when cavitation occurred. Lu et al. (2017b) noticed that there is a clear correspondence between the development of cavitation and the enhancement of

vibration signals during the decline of NPSHa when studying the vibration characteristics caused by cavitation of centrifugal pumps, shown in Fig. 15. The research in (Černetič, 2009; Čudina and Prezelj, 2009) revealed that the cause of vibration caused by cavitation is because the collapse of bubbles in the blade passage during cavitation will produce unsteady impact and shock on the surface of the blade, which is then transmitted to other locations of the pump through the fluid, leading to the pump's vibrational energy increasing rapidly. It was found that the vibration-induced vibration in the pump is most affected at the pump inlet, which maybe because cavitation is the strongest at the leading edge of the blade (Lu et al., 2017a). The asymmetry of the airfoil on the impeller causes vibration of the impeller shaft (Yoshida et al., 2010).

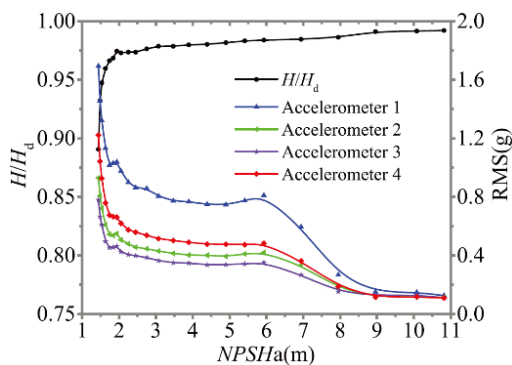


Fig. 15 Root mean square (RMS) of vibration and the suction performance curve

Reprinted from (Lu et al., 2017a), Copyright 2017, with permission from Springer Science+Business Media

Pressure pulsation is another major cause of vibration and noise, so the factors that stimulate pressure pulsation are also the factors that stimulate vibration and noise. At present, the mechanism of pressure pulsation is further explored mainly by studying the vibration and noise caused by pressure pulsation. Researchers have studied the mechanism of pressure fluctuation. When the fluid flows out of the trailing edge of the blade, the vortex caused by the trailing edge contributes to flow instability, and the fluid will collide with the tongue and the volute wall, resulting in strong turbulence (Choi et al., 2003; Barrio et al., 2011). Strong pressure pulsations charac-

terized by discrete blade passing frequencies and harmonics are thus generated (Parrondo-Gayo et al., 2002). Wang K et al. (2016) also found that the frequency of pressure pulsation at each monitoring point on the pump is mainly the axial frequency and multi-axis frequency, which confirmed that the interaction between the blade and the tongue is the main cause of pressure fluctuation.

When the flow rates are different, the causes of pressure pulsation are diversified (Zheng et al., 2018). Under the condition of large flow rate, pressure fluctuation is mainly caused by the relative motion of the blade and the volute tongue and the low pressure of the rear edge of the blade. Under the condition of small flow rate, the pressure fluctuation is mainly related to the relative position of the blade and the volute tongue and the vortex structure at the outlet of the blade.

Chalghoum et al. (2018) and Zhang JF et al. (2019) studied the distribution of pressure fluctuations in centrifugal pumps by numerical simulation and experiments. It can be explained that the instability of the internal flow field of the centrifugal pump is the main reason for the pressure fluctuation of the centrifugal pump. According to the simulation results of the pressure fluctuation distribution, it was found that there is a maximum pressure fluctuation distribution caused by the rotor-stator interaction in the volute tongue region, as displayed in Fig. 16. Additionally, rotational stall can also contribute to pressure fluctuation under off-design conditions (Zhao et al., 2018). Compared with single-suction centrifugal pumps, double-suction centrifugal pumps tend to suffer from more pressure fluctuations because of the high energy involved (Yao et al., 2011). The pressure fluctuations in most regions of the volute are obtained by superimposing the pressure generated by the two impellers, except for the region of axial flows (Song et al., 2019).

In addition to cavitation and pressure pulsations, other factors can contribute to vibration and noise in the centrifugal pump. Under high flow conditions, local low pressure at the tongue of the volute produces backflow and results in high-speed jets, which cause more severe vibration (Zhao and Zhao, 2018; Lu et al., 2019; Tong ZM et al., 2019a). At a lower flow rate, the unsteady flow in the pump is more

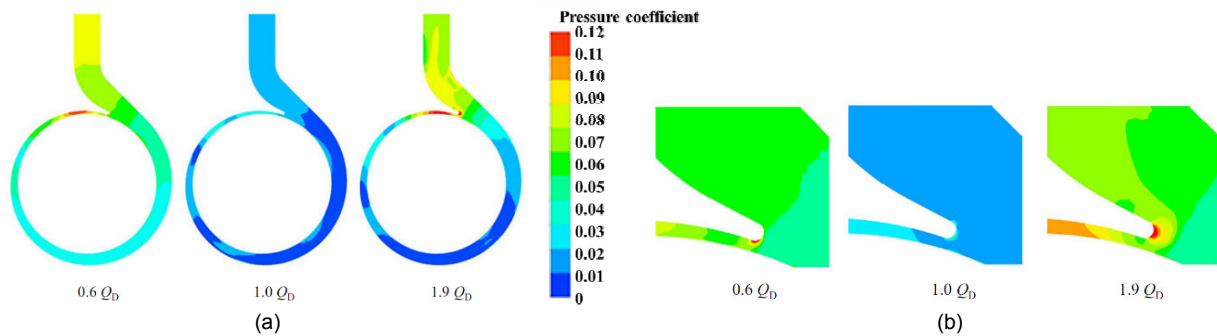


Fig. 16 Pressure pulsation in the volute flow passage (Zhang JF et al., 2019)
(a) Entire volute; (b) Enlarged tongue region

obvious, the vibration and noise at this time are more prominent, and the vibration frequency at this time is concentrated in the low frequency region. For the solid-liquid two-phase flow, the amplitude of the vibration is strongly influenced by the concentration, and increases with the increase of the concentration (Zhao and Zhao, 2018).

In general, the source of centrifugal pump vibration and noise can be summarized as a hydrodynamic source and a mechanical source (Kim et al., 2013; Goyal and Pabla, 2016; Wang K et al., 2018; Guo et al., 2019; Mousmoulis et al., 2019). The hydrodynamic source involves flow characteristics within the pump, such as turbulence, secondary flow, water hammer, cavitation, interaction of the impeller with the volute, and strong interaction of the impeller with the surrounding fluid. Mechanical sources include non-uniform forces between the rotating and non-rotating components of the pump system, improper use of the pump as specified in the installation manual, and conditions caused by incorrect pump assembly and wear.

4.2 Diagnosis based on vibration and noise

Farokhzad et al. (2013) revealed that the changes in vibration signals were a function of failure under different operating conditions. Gao et al. (2017) observed the characteristics of the vibrational energy and found that the vibration signal works better than the traditional 3% head drop rule when detecting the occurrence of cavitation. Therefore, it is feasible to use the vibration and noise signals for centrifugal pump fault detection.

In addition, fault diagnosis based on vibration signals is a non-invasive diagnostic method, which

will not affect the integrity of the centrifugal pump (Lu et al., 2019). The vibration signals can be used to effectively detect the hump, rotation stall, secondary flow, unstable flow, and cavitation. Among these faults mostly detected by vibration and noise is cavitation (Luo et al., 2015; Li Y et al., 2018; Al-Obaidi, 2019). At present, vibration signals are mostly used in fault diagnosis. However, in recent research, it has been found that, compared with solid vibration and air noise methods, fault diagnosis methods based on liquid noise in non-small pumps are more sensitive and reliable (Dong et al., 2019). Fig. 17 depicts the normalized 1/3 octave spectrum of liquid noise in Dong et al. (2019)'s experiment.

It is a relatively new trend to apply artificial intelligence to fault detection based on vibration signal, which has been studied by several scholars in recent years. Sakthivel et al. (2010b) collected the vibration signals of the monoblock centrifugal pump in six kinds of fault states, and extracted and classified the characteristics of the vibration signal using the C4.5 decision tree algorithm for fault diagnosis. Sakthivel et al. (2010b)'s research proves the practicality of applying the C4.5 decision tree algorithm to monoblock centrifugal pump fault diagnosis. Sakthivel et al. (2010a) also compared the application of the decision tree fuzzy method and rough set fuzzy method in centrifugal pump fault classification under the same experimental conditions. The results showed that the decision tree fuzzy hybrid system somewhat better performed than the rough set fuzzy hybrid system in terms of overall classification accuracy.

Bordoloi and Tiwari (2017) used a support vector machine (SVM), a machine learning tool, to extract statistical features from vibration signals to diagnose

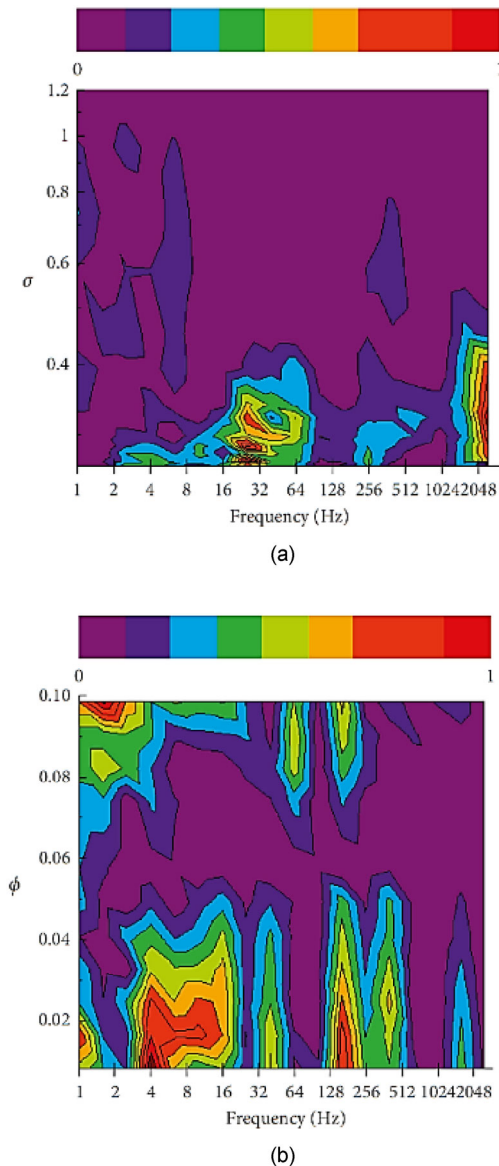


Fig. 17 Normalized 1/3 octave spectrum of liquid-borne noise (Dong et al., 2019)

(a) Under various cavitation coefficients σ ; (b) Under various flow coefficients ϕ

blockage levels and cavitation problems at different flow rates. Al Tobi et al. (2017) invented a centrifugal pump fault diagnosis method based on artificial intelligence and a genetic algorithm system. This method uses vibration analysis and automatic diagnostic methods to analyze the vibration mode of the centrifugal pump to judge the failure. Zouari et al. (2004) used neural networks and fuzzy neural networks to diagnose centrifugal pump faults, and uti-

lized statistical methods and spectrum analysis for feature extraction. Panda et al. (2018) installed the centrifugal pump in a machine fault simulator for experiments to obtain the vibration characteristics of the pump. A machine learning algorithm based on support vector machines was used to study fluid blockage and cavitation failure at different flow rates. In these experiments, Panda et al. (2018) found that binary fault classification performed better than various fault classifications in predicting different congestion situations. A multi-class support vector machine fault classification algorithm based on hyperparameter optimization was later proposed (Rapur and Tiwari, 2018). Fig. 18 is the flowchart of classification methodology. The state of the centrifugal pump was monitored using the vibration power spectrum of the centrifugal pump and the current data of the induction motor line. According to these experimental results, this method can successfully classify both multiple independent faults and coexisting faults (Li Y et al., 2018).

4.3 Signal processing

The usual means for analyzing the pressure signal gathered include time-domain analysis, frequency domain analysis, and time frequency domain analysis. The time-domain analysis method can obtain the change law of the amplitude value with time, and the frequency-domain analysis method can obtain the individual sub-signals of the synthesized total signal, both of which can be used to assist fault analysis. The two methods are the most basic and popularly used, so this paper will not go into too much description here but rather will introduce signal analysis methods in the time-frequency domain.

The time-frequency domain analysis method makes up for the shortcomings of time-domain and frequency-domain analyses and can represent both time-domain and frequency-domain features. Researchers have used a variety of time-frequency domain analysis methods in the processing of centrifugal pump vibration signals or pressure pulsation signals. Compared with traditional frequency domain analysis, short-time Fourier transform (STFT) offers better time resolution and can be used to analyze vibration signal. Li Y et al. (2018) analyzed the vibration signal using an ameliorative algorithm, i.e.

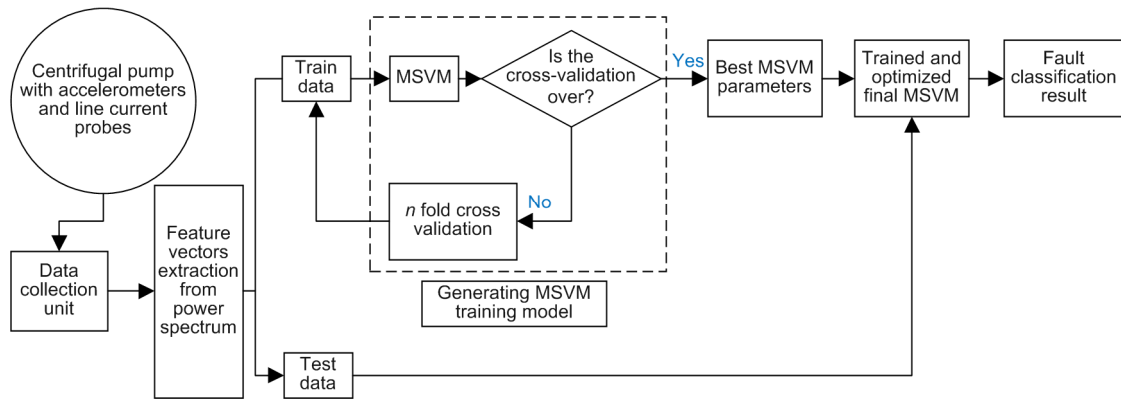


Fig. 18 Process of the classification methodology

MSVM is the multi-class support vector machine. Reprinted from (Rapur and Tiwari, 2018a), Copyright 2018, with permission from Springer Science+Business Media

united algorithm based on STFT and Wigner-Ville distribution (WVD). Fig. 19a shows the time domain information of the vibration signal $x(t)$. The WVD result of $x(t)$ is shown in Fig. 19b. Fig. 19c depicts the result of the STFT of $x(t)$. Fig. 19d describes the result of STFT-WVD of $x(t)$. By comparing the four figures, it can be concluded that STFT-WVD is excellent in denoising, time-frequency concentration, and eliminating cross terms. However, this method is limited in time and frequency resolution and time frequency aggregation (Luo et al., 2019).

The advent of wavelet analysis solved this problem. Pavesi et al. (2008) and Cavazzini et al. (2011) proved the applicability of wavelet in the field of impeller machinery. Wavelet analysis can provide high frequency resolution in the low frequency band of the signal, improve time resolution in the high frequency band, and perform noise reduction on some original signals (Al Tobi et al., 2017). This powerful function makes the wavelet transform increasingly popular in the field of centrifugal pump fault diagnosis (Bordoloi and Tiwari, 2017). An adaptive optimal-kernel time-frequency representation (AOK TFR) is another means for signal analysis in the time-frequency domain and the time-frequency domain for a double-suction centrifugal pump was first identified in this time-frequency method (Yao et al., 2011). Sun et al. (2018) used a time-frequency signal analysis method based on the cyclic stationary theory to detect cavitation and seal failure of centrifugal pumps. The time-frequency signal analysis method based on the cyclic stationary theory is able to extract the frequency characteristic components of the signal from

the non-stationary vibration signal while avoiding the influence of the modulation and noise components on the vibration signal, thereby performing fault diagnosis.

5 Performance optimization of centrifugal pumps

Optimized pump design is one of the primary ways to achieve excellent pump performance (Hergt, 1999). In recent years, various optimization techniques have been combined with CFD to improve the performance of centrifugal pumps (Zhao et al., 2016).

Some scholars have optimized the volute (Golbabaei Asl et al., 2009), the nozzle (Chang et al., 2020), and the number of supporting blades (Guleren, 2018; Xue et al., 2019) to improve the performance of centrifugal pump. The impeller is the most important part of centrifugal pump as its geometry is closely related to the performance of the pump. Therefore, the optimization of the shape of the impeller should be carefully considered (Zhang et al., 2014a).

In previous studies, designers often studied the effects of a single variable of impeller blades on efficiency, such as different blade winding angles (Tan et al., 2014a; Gao et al., 2016), number of blades (Bellary et al., 2016; Wei et al., 2017), and blade exit width (Shi et al., 2013), or by determining the optimum geometry of the blade to achieve higher efficiency. Obviously, these studies only regard the energy efficiency of centrifugal pumps as a single

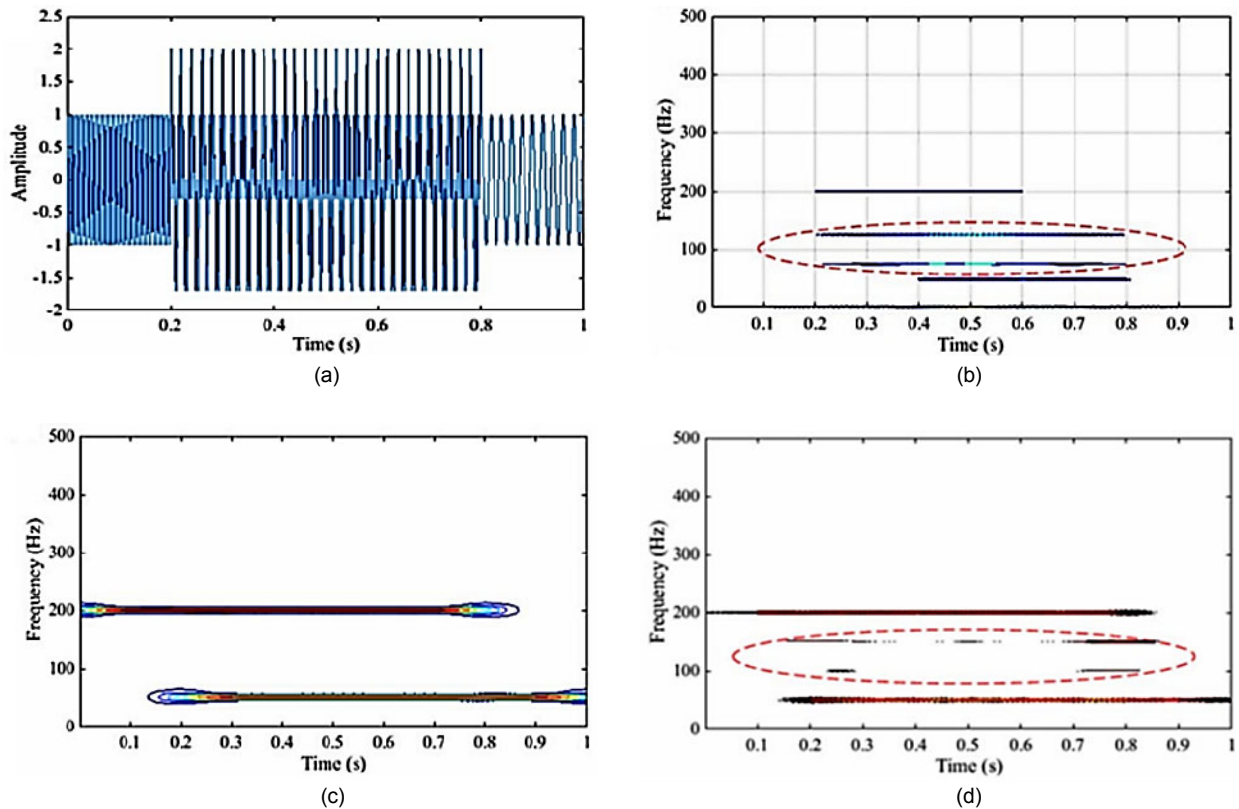


Fig. 19 Time domain diagram and the calculation results of three algorithms of the signal $x(t)$

(a) Time domain diagram of signal $x(t)$; (b) Calculation result of WVD method; (c) Calculation result of STFT method; (d) Calculation result of STFT-WVD method. Reprinted from (Li Y et al., 2018), Copyright 2018, with permission from Springer Science+Business Media

objective of design and optimization while ignoring other performance indices such as head and NPSHr. Although efficiency is always the most important economic and technical index of the pump, other performance parameters also determine whether the pump can run stably and efficiently (Zhang et al., 2014a). Therefore, the impeller optimization design of a centrifugal pump is a multi-objective optimization problem with multiple design requirements.

In fact, the head and efficiency need to be maximized, while the NPSHr needs to be minimized, and these optimization parameters cannot be achieved simultaneously. In addition, these three performance indices are often obtained through experimental tests or CFD simulation. In order to achieve an objective optimization, a large amount of external characteristic data need to be obtained under different working conditions (Bellary et al., 2016), requiring a significant investment of time.

For the impeller of the centrifugal pump, there should be more than 14 parameters to completely describe the entire geometric information (Liu et al., 2018). One of the most difficult problems in impeller geometric parameterization is to reduce design variables as much as possible while satisfying design requirements. It can be challenging to reasonably evaluate these variables and make effective values (Zhou et al., 2012; Tong SG et al., 2018).

The most popular optimization method at present is to combine the design of experiment (DOE), the surrogate model, and the multi-objective optimization algorithm. This method better overcomes the above shortcomings in the actual optimization of the centrifugal pump. It enables the optimal combination for finding parameters, establishing an appropriate metamodel between decision variables and related objective functions, and determining the best compromise among several controversial goals.

As shown in Fig. 20, the entire process mainly includes the following steps:

1. Use DOE to determine the design variables for performance-sensitive responses. Generate different impeller solutions.

2. According to the design variables, use CFD software to simulate a group of centrifugal pumps with different blade shapes. Obtain simulation results of head, efficiency, NPSHr, and other objective performance parameters.

3. Use a surrogate model to establish the relationship between design parameters and objective

parameters. The design parameters are used as input variables for the surrogate model, and the objective parameters are used as output variables.

4. Test and verify the surrogate model constructed in Step 3. The predicted value is then compared with the simulation value. If the predicted value is in good agreement, Step 5 is entered. Otherwise, go back to Step 3 to update the surrogate model.

5. Apply the multi-objective optimization (MOO) algorithm to solve the multi-objective optimization problem of centrifugal pump based on the surrogate

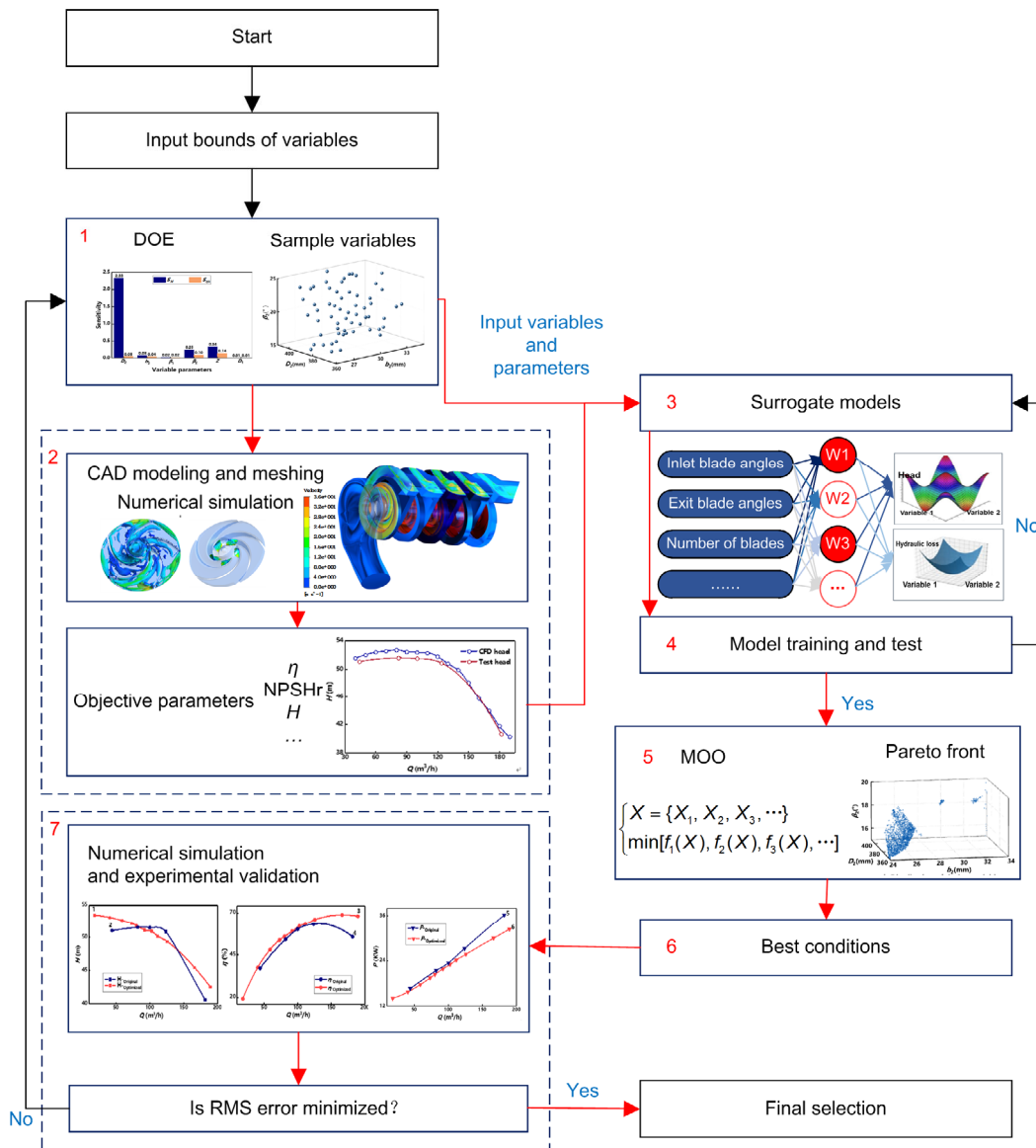


Fig. 20 Typical performance optimization process of centrifugal pumps

model, and obtain the Pareto front.

6. Select the final solution from Pareto front as the optimal solution.

The centrifugal pumps are generated based on the values of design variables provided by the best solution. Finally, the CFD simulation of the optimized model of the centrifugal pump was carried out, and it was verified with the substitute model and experimental results.

5.1 Design of experiment

DOE is the basis of optimization. Using this method, the importance of design variables relative to the optimization objective can be calculated, and the optimal combination of design variables can be obtained (Pei et al., 2016b), which can effectively improve the performance of the pump and shorten the design cycle (Pei et al., 2019). Smaller alternative model errors can be obtained using DOE samples compared to using the same number of random samples (van den Braembussche, 2008).

Orthogonal array (OA) and optimized Latin hypercube sampling (OLHS) are common design methods. The OLHS method is an improvement on the Latin hypercube sampling method (Pei et al., 2016b, 2019). OA is a DOE method that evolved from Latin hypercube design and group theory (Zhao et al., 2016). In the orthogonal experiment, representative experiments can be selected from the overall experiment to help determine the optimal solution and reveal important information that was not expected (Zhou et al., 2013). OA minimizes the number of test runs while maintaining a pair of balanced attributes (Nataraj and Arunachalam, 2006). Several scholars have used orthogonal methods for the design of centrifugal pumps (Zhou et al., 2013; Zhang et al., 2017; Wang and Huo, 2018; Wang et al., 2019).

A matrix analysis model was proposed (Si et al., 2013). The effects of 10 geometric parameters of the impeller and vane on the head, efficiency, and shaft power were studied. The order of each variable was directly determined according to weight. Finally, a set of optimal geometric parameters was obtained by weighting calculation. The proposed method solves the problem of large calculation amount and unreasonable weight determination in orthogonal experimental design.

5.2 Surrogate model

Establishing a surrogate model can greatly reduce computational pressure (Zhao et al., 2016). Artificial neural network (ANN) (Wu et al., 2008; Derakhshan et al., 2013), response surface analysis (RSA) (Pei et al., 2016a), Kriging (KRG) (Zhang et al., 2014c), and radial basis neural network (RBNN) (Bellary et al., 2016) have all been applied in centrifugal pump optimization.

RSA is a polynomial function of the response generated by numerical calculations (Pei et al., 2016a). ANN abstracts the human brain's vegetative cell network from the angle of data process, establishes an easy model, and forms completely different networks that are in step with different affiliation strategies (Wang et al., 2019). The KRG model has a global model and system deviation at non-sampling points (Bellary et al., 2016). Compared with RSA, the KRG method has advantages in high-dimensional nonlinear problems and prediction accuracy due to the use of random hypothesis, especially in multi-objective optimization problems (Zhang et al., 2014c). The basic concepts of ANN and RBNN are all derived from learning events. However, compared with ANN, the RBNN algorithm implementation is relatively simple, and in most cases RBNN algorithm is superior to the other three surrogate models in accuracy and robustness (Jin et al., 2001). Heo et al. (2016) compared the accuracy of RSA, KRG, and RBNN in the prediction of centrifugal pump performance and verified that the optimal objective function was predicted by the RBNN model.

Reliability and robustness can be improved by using multiple surrogates, as surrogates are problem-dependent (Siddique et al., 2018). The weighted average surrogate (WAS) is based on the average of the predicted error sum of squares (PRESS), which is implemented from cross validation (CV) error estimations (Bellary et al., 2016). A simplified form of the predictive response of the WAS model can be written as

$$F_{\text{WAS}} = w_{\text{RSA}} F_{\text{RSA}} + w_{\text{KRG}} F_{\text{KRG}} + w_{\text{RBNN}} F_{\text{RBNN}}, \quad (1)$$

where F_{RSA} , F_{KRG} , and F_{RBNN} are constructed using the CFD evaluated responses. w_{RSA} , w_{KRG} , and w_{RBNN} represent weights. When the surrogate model has a

lower CV error, it will have a higher weight, meaning that the lower the CV error, the greater the contribution of the surrogate model to the construction of the WAS model (Bellary et al., 2016). Since WAS includes predictions for all surrogate models, satisfactory results have been obtained. Therefore, the authors suggest using multiple surrogates to generate the Pareto front instead of using a single agent.

5.3 Multi-objective optimization

MOO usually maximizes or minimizes two or more objective functions under variable constraints (Pei et al., 2019). It is almost impossible to obtain an optimal solution that satisfies all objective functions. The multiple parameters considered are a “win-win” strategy to satisfy as many opposing goals as possible at the same time.

The genetic algorithm achieves global optimization of space through population evolution based on coding design parameters, cross-genetic and offspring mutations (Liu et al., 2019). Zhu et al. (2012) used genetic algorithm to predict the performance of centrifugal pump, which reduced the sample training time compared with the back propagation (BP) network prediction algorithm and was more suitable for engineering applications. Safikhani et al. (2011) and Huang et al. (2015) used a multi-objective genetic algorithm (MOGA) to optimize the impeller of the pump, and both algorithms obtained good results.

Non-dominated sorting genetic algorithm-II (NSGA-II) was developed to reduce time and complexity and improved convergence to the optimal Pareto front (Fang et al., 2008; Tong SG et al., 2019). Zhang et al. (2011) combined ANN and NSGA-II to develop a multi-objective pump impeller optimization method, which improves the pressure and efficiency of the spiral shaft multiphase pump. Benturki et al. (2018) obtained an optimal design from two Pareto fronts through CFD and NSGA-II, as shown in Fig. 21. CFD analysis was carried out on the optimal multistage pump, and the optimized two-stage centrifugal pump's meridional shape was changed. By comparing the internal flow field, the hydrodynamic performance demonstrated greater performance in flow stability, pressure loading and recovery, as shown in Fig. 22. The performance of multistage pump was also improved.

NSGA-III algorithm was proposed by Deb and Jain (2014). NSGA-III introduces the concept of reference points based on NSGA-II algorithm, which improves the convergence of the algorithm and the uniformity of the optimal solution distribution. We used NSGA-III and NSGA-II to optimize the impeller structure of the centrifugal pump separately. By comparing the pump head, efficiency, and flow field streamline distribution optimized by the two algorithms, we find that the overall performance of the NSGA-III algorithm is superior (Tong ZM et al., 2019b).

Multi-objective evolutionary algorithm (MOEA/D) is a scaling function that uses uniformly distributed weight vectors (Zhang and Li, 2007). MOEA/D has good global search performance and can better deal with multi-objective problems involving multiple conflicting objectives. Based on the multi-objective evolutionary algorithm, Zhang et al. (2014a) used Pareto optimal solution to optimize the impeller of the multi-phase pump with spiral axis. Bonaiuti and Zangeneh (2009) not only considered multiple objectives, but also optimized performance at multiple operating points under different operating conditions.

In the research of MOO of centrifugal pump, MOGA and NSGA-II have been widely used. Eagle strategy (ES) (Derakhshan and Bashiri, 2018), artificial bee colony (ABC) (Derakhshan et al., 2013), multi-island genetic algorithm (MIGA) (Wang WJ et al., 2017), artificial fish swarm algorithm (AFSA) (Liu et al., 2019), and particle swarm optimization (PSO) (Wang YQ et al., 2018) have also been used for MOO of pumps. From the perspective of solving practical centrifugal pump problems, exploring more suitable MOO methods based on constraints is still a focus of current research.

5.4 Performance optimization of centrifugal pumps

Methods to improve the performance of centrifugal pump by combining DOE, surrogate model, and MOO algorithm have been widely applied. Table 3 (p.106) summarizes the use of design parameters, surrogate model, and optimization methods in previous studies. Various shape optimization parameters and objective parameters are shown in Fig. 23 (p.107).

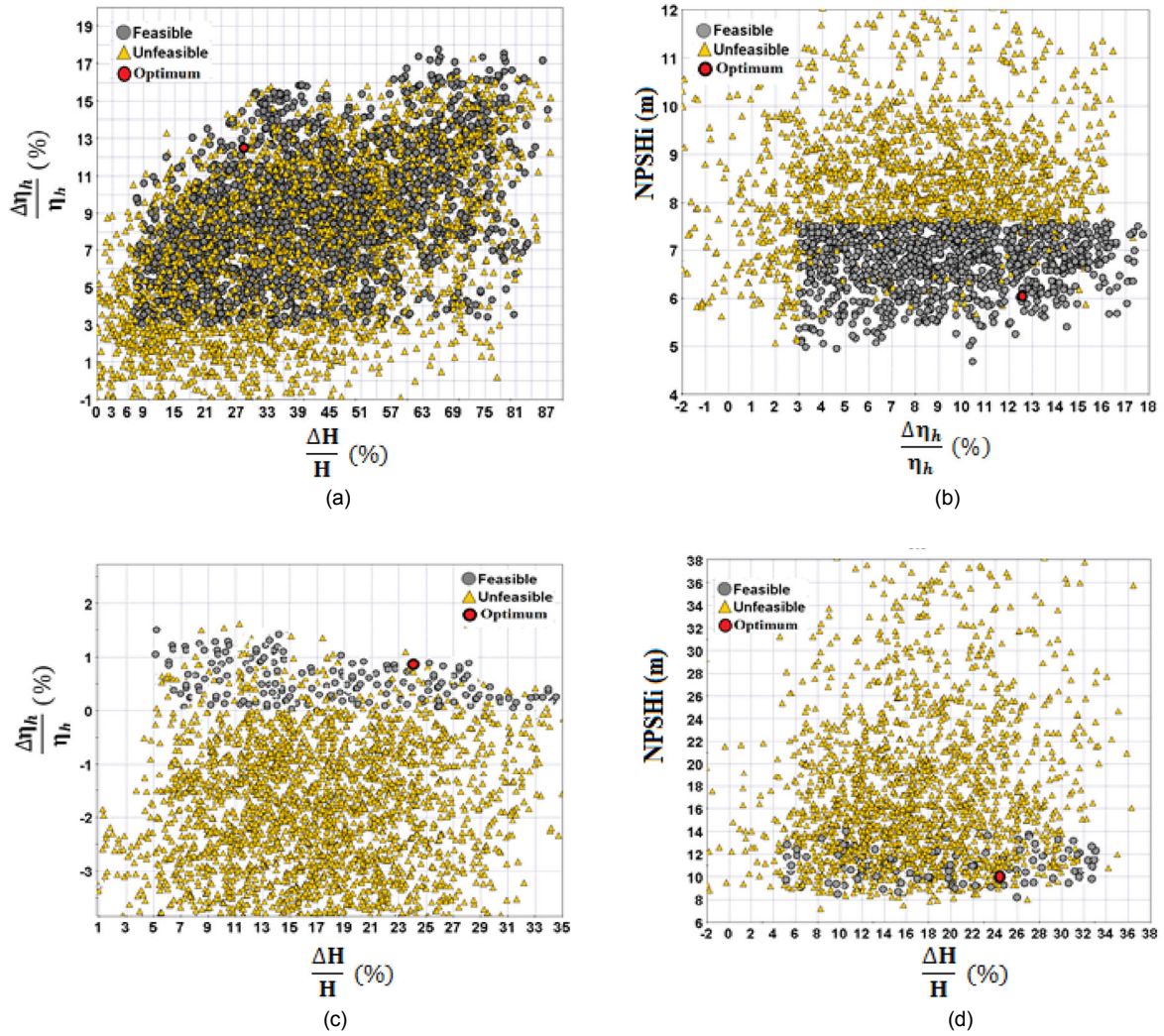


Fig. 21 Pareto fronts of the first stage: (a) head and hydraulic efficiency, (b) hydraulic efficiency and NPSHi; Pareto fronts of the second stage: (c) head and hydraulic efficiency, (d) head and NPSHi (Benturki et al., 2018)

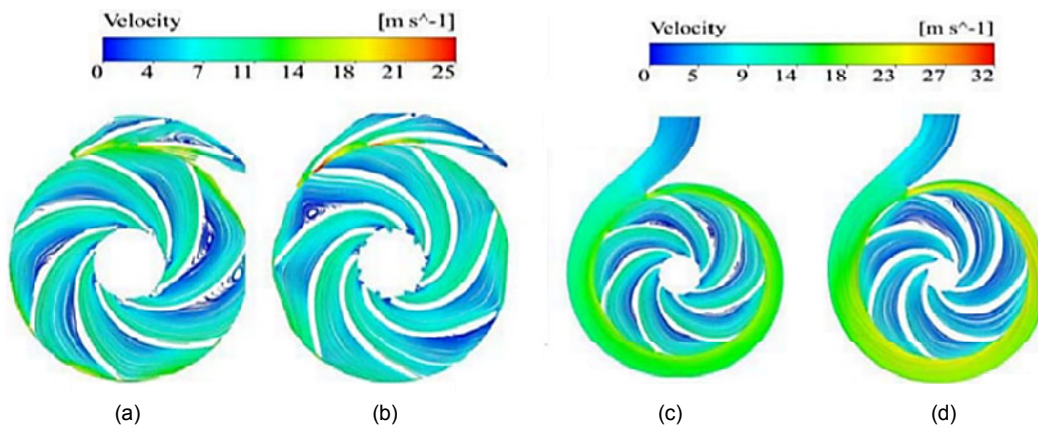


Fig. 22 Mid-span streamlines colored by the relative flow velocity (a) Original first stage; (b) Optimum first stage; (c) Original second stage; (d) Optimum second stage (Benturki et al., 2018)

Table 3 Summarized previous studies on centrifugal pump optimization

Reference	Variable parameter	Surrogate model	Optimization algorithm	Optimization parameter
Nourbakhsh et al., 2011	Leading edge angle, trailing edge angle, stagger angle	GMDH-type neural network	PSO	NPSHr, efficiency
Safikhani et al., 2011	Leading edge angle, trailing edge angle, stagger angle	GMDH-type neural network	Pareto MOO	Efficiency, NPSHr
Wang et al., 2011	Meridional sweep at hub, meridional sweep at tip, tangential lean at hub, tangential lean at tip	Back propagation neural network (BPNN)	NSGA-II	Aerodynamic performance, efficiency, total pressure, choked mass flow
Zhang et al., 2011	Flange import angle, flange outlet angle, half cone angle of hub, hub ratio of import	BP-ANN	NSGA-II	Head, efficiency
Derakhshan et al., 2013	Hub diameter, suction diameter, impeller diameter, impeller width, inlet and outlet blade angles	ANN	ABC	Efficiency, head
Yang and Xiao, 2014	Impeller high pressure side diameter, impeller low pressure side shroud diameter, impeller low pressure side hub diameter, impeller high pressure side exit width	RSA	MOGA	Turbine performance at the design point and low flow rate of the rated point
Zhang et al., 2014b	Four design variables for the Bezier curve	KRG	NSGA II, MOEA/D	Efficiency, NPSHr
Kim et al., 2015	Inlet angle of the impeller hub, inlet angle of the impeller shroud, outlet angle of the impeller hub, outlet angle of the impeller shroud	RSA		Head, efficiency
Heo et al., 2016	Hub inlet angle, first control point of a fourth-order Bezier curve defining hub on the meridional plane of impeller, blade outlet angle, blade angle profile coefficient of impeller	RSA, KRG, RBNN	Sequential quadratic programming (SQP)	Efficiency, head
Pei et al., 2016a	Shroud radius of arc, hub radius of arc, shroud angle, hub angle	RSA	NSGA-II	Efficiencies based on the design points of $0.6Q_0$, $1.0Q_0$, and $1.62Q_0$
Shim et al., 2016	Expansion coefficient of the rib structure, ratio of the distance between the rib starting point and the volute entrance to the diameter of impeller, ratio of the angle from the volute throat to the end of the rib structure to the angle of the entire discharge diffuser	RSA	MOGA	Radial force, amplitude of the radial force fluctuation
Zhao et al., 2016	Blade outlet angle, blade inlet angle, splitter offset angle, impeller meridional section	Two-layer feed-forward neural network	NSGA-II	Efficiency, NPSHr
Derakhshan and Bashiri, 2018	Hub diameter, suction diameter, impeller diameter, impeller width, inlet and outlet blade angles	ANN, feedforward neural network	ES	Efficiency, head
Shim et al., 2018	A fifth-order Bezier curve for the shroud, ratio of the inlet radius of the blade hub to the inlet radius of the impeller shroud, coefficients for determining the incidence angles at the shroud, ratio of the axial length of the blade to the inlet radius of the impeller shroud	KRG	MOGA	Efficiency, NPSHr
Tao et al., 2018b	Blade angle, wrap angle on hub, mid-span, shroud	ANN	Pareto MOO	Efficiency, head

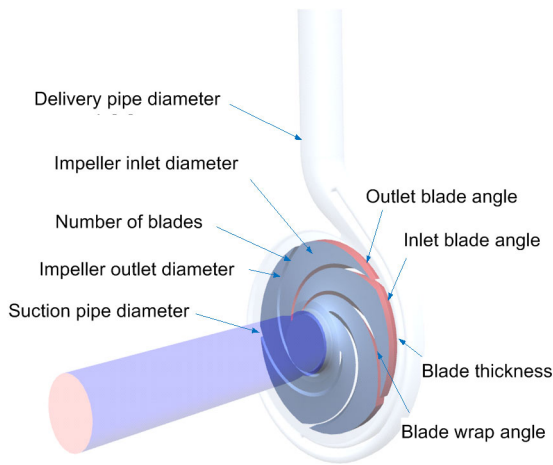


Fig. 23 Centrifugal pump impeller design variables and optimization parameters

Inlet blade angle, outlet blade angle, and the number of blades are the main sensitive variables that affect the performance of the centrifugal pump, and thus they are selected as design variables in most studies. The decrease of inlet angle and increase of outlet angle can improve the performance of centrifugal pump in treating viscous fluid (Tao et al., 2018b). The outlet blade angle is also an important design parameter that increases peripheral velocity (Siddique et al., 2018). Tong ZM et al. (2019c) explored the optimization of the design value of guide vane outlet flow angle based on the matching of rotor loss characteristics with specified variable operating conditions. With the increase in the number of blades, the flow line tends to be uniform and the pump head increases (Liu et al., 2010). However, contrary to Liu et al. (2010)'s opinion, it is believed that increasing the number of blades increases the blockage at the inlet of the pump, leading to the decrease of head and efficiency (Cavazzini et al., 2015).

The Bezier curve technology can make the angle of blade profile arbitrary change and keep stable, so using the Bezier curve control point to optimize impeller blade shape has been widely used in recent years (Goel et al., 2008; Pei et al., 2016b). Based on the non-uniform rational B-spline (NURBS) 3D reconstruction method, the aerodynamic optimization design of centrifugal impeller blade was carried out (Liu and Zhang, 2010). Using the Bezier curve and linear function to control the annular angle distribution and the stacking angle of blade profile, the op-

timal alternative model of blade shape was determined, and the hydraulic efficiency was significantly improved (Liu et al., 2019).

Head, efficiency, and NPSHr are the primary objective functions in most studies (Bellary et al., 2016; Zhao et al., 2016; Wang YQ et al., 2018; Liu et al., 2019). Pei et al. (2019) took another approach, taking the efficiency of centrifugal pump at $0.5Q_0$, $1.0Q_0$, and $1.5Q_0$ as the objective function, and proposing a MOO method based on genetic algorithm and ANN. Under the three optimization conditions, the velocity distribution of inlet and outlet was more uniform than that of the original condition, which expanded the range of efficient operation of the centrifugal pump (Pei et al., 2019).

6 Conclusions

This review paper focuses on the latest developments in the internal flow field and external characteristics of centrifugal pumps, performance optimization, and fault detection:

1. The research on the internal flow structure of centrifugal pumps in the literature published in recent years was reviewed. We discussed the numerical methods and visual experimental techniques for the flow field in centrifugal pumps. The development and genesis of various flow structures in the pump under gas-liquid two-phase state and cavitation state have been discussed or partially discussed. For the numerical simulation method, the algorithm for the flow field calculation in the centrifugal pump can be further improved, which will make the convergence better, the stability condition more relaxed, and the calculation time shorter, and improve the design efficiency.

2. A summary of the external characteristics of the centrifugal pump under non-design conditions was provided, in addition to an explanation of the complex relationship between the development of cavitation and external features and the influence of overcurrent components on external characteristics.

3. There are many reasons for pressure pulsation in centrifugal pumps, among which the interaction between rotor and stator is the main reason under all operation conditions. In the case of large flow rate, the pressure fluctuation is also related to the low

pressure of the trailing edge of the blade. Under the condition of small flow rate, the pressure fluctuation results from the vortex structure at the outlet of the blade as well. There are many optimization methods for reducing pressure, including impeller optimization, diffuser optimization, and distance optimization between impeller and volute. The essence of these optimization methods is to stabilize the flow in centrifugal pump.

4. The various methods and measures for optimizing the performance of centrifugal pumps are described in detail. The latest overall process for multi-objective optimization of centrifugal pumps was reviewed. The applicability of various alternative models and multi-objective optimization methods to optimize the performance of centrifugal pumps was introduced and analyzed. A summary of the design variables and optimization parameters for multi-objective optimization of centrifugal pumps in recent years to further promote the optimization research of centrifugal pumps was provided.

At present, the rapid development of experiments and numerical techniques has enabled researchers at home and abroad to make progress in the study of the internal flow phenomenon mechanism and flow field structure of centrifugal pumps. However, there is no systematic and rapid method to accurately predict centrifugal pump noise, cavitation, backflow, secondary flow, and other phenomena and optimize the centrifugal pump structure. There are still some problems to be solved in the research, such as the monitoring and prevention of primary cavitation, how the rotational stall phenomenon in the pump develops, and data differences that cannot be ignored between the numerical and experimental results. Therefore, the coupling relationship between the complex unsteady flow characteristics of the fluid in the centrifugal pump and the pump performance is worthy of study. To further improve the efficiency of centrifugal pumps in the future, researchers are encouraged to focus on developing multi-dimensional visualization technology to measure the internal flow field as well as advanced numerical models based on high-performance computing facilities.

Contributors

Zhe-ming TONG and Jia-ge XIN designed the research and wrote the first draft of the manuscript. Shui-guang TONG and Zhong-qin YANG processed the data. Shui-guang TONG,

Jian-yun ZHAO, and Jun-hua MAO revised the final version and provided funding support.

Conflict of interest

Zhe-ming TONG, Jia-ge XIN, Shui-guang TONG, Zhong-qin YANG, Jian-yun ZHAO, and Jun-hua MAO declare that they have no conflict of interest.

References

- Alemi H, Nourbakhsh SA, Raisee M, et al., 2015. Effects of volute curvature on performance of a low specific-speed centrifugal pump at design and off-design conditions. *Journal of Turbomachinery*, 137(4):041009. <https://doi.org/10.1115/1.4028766>
- Al-Obaidi AR, 2019. Investigation of effect of pump rotational speed on performance and detection of cavitation within a centrifugal pump using vibration analysis. *Heliyon*, 5(6):e01910. <https://doi.org/10.1016/j.heliyon.2019.e01910>
- Al Tobi MAS, Bevan G, Ramachandran KP, et al., 2017. Experimental set-up for investigation of fault diagnosis of a centrifugal pump. *International Journal of Mechanical, Aerospace, Industrial, Mechatronic and Manufacturing Engineering*, 11(3):481-485.
- Ayad AF, Abdalla HM, Aly AAEA, 2015. Effect of semi-open impeller side clearance on the centrifugal pump performance using CFD. *Aerospace Science and Technology*, 47:247-255. <https://doi.org/10.1016/j.ast.2015.09.033>
- Bachert R, Stoffel B, Dular M, 2010. Unsteady cavitation at the tongue of the volute of a centrifugal pump. *Journal of Fluids Engineering*, 132(6):061301. <https://doi.org/10.1115/1.4001570>
- Barrio R, Parrondo J, Blanco E, 2010. Numerical analysis of the unsteady flow in the near-tongue region in a volute-type centrifugal pump for different operating points. *Computers & Fluids*, 39(5):859-870. <https://doi.org/10.1016/j.compfluid.2010.01.001>
- Barrio R, Fernández J, Blanco E, et al., 2011. Estimation of radial load in centrifugal pumps using computational fluid dynamics. *European Journal of Mechanics-B/Fluids*, 30(3):316-324. <https://doi.org/10.1016/j.euromechflu.2011.01.002>
- Barrios L, Prado MG, 2011. Experimental visualization of two-phase flow inside an electrical submersible pump stage. *Journal of Energy Resources Technology*, 133(4):042901. <https://doi.org/10.1115/1.4004966>
- Bellary SAI, Adhav R, Siddique MH, et al., 2016. Application of computational fluid dynamics and surrogate-coupled evolutionary computing to enhance centrifugal-pump performance. *Engineering Applications of Computational Fluid Mechanics*, 10(1):171-181. <https://doi.org/10.1080/19942060.2015.1128359>
- Benaouicha M, Astolfi JA, Ducoin A, et al., 2010. A numerical

- study of cavitation induced vibration. Proceedings of ASME Pressure Vessels and Piping Division/K-PVP Conference, p.35-42.
- Benim AC, Pasqualotto E, Suh SH, 2008. Modelling turbulent flow past a circular cylinder by RANS, URANS, LES and DES. *Progress in Computational Fluid Dynamics, An International Journal (PCFD)*, 8(5):299-307.
<https://doi.org/10.1504/Pcfd.2008.019483>
- Bensow RE, Bark G, 2010. Implicit LES predictions of the cavitating flow on a propeller. *Journal of Fluids Engineering*, 132(4):041302.
<https://doi.org/10.1115/1.4001342>
- Benturki M, Dizene R, Ghenaïet A, 2018. Multi-objective optimization of two-stage centrifugal pump using NSGA-II algorithm. *Journal of Applied Fluid Mechanics*, 11(4):929-942.
<https://doi.org/10.29252/jafm.11.04.28509>
- Bilus I, Predin A, 2009. Numerical and experimental approach to cavitation surge obstruction in water pump. *International Journal of Numerical Methods for Heat & Fluid Flow*, 19(7):818-834.
<https://doi.org/10.1108/09615530910984091>
- Bonaiuti D, Zangeneh M, 2009. On the coupling of inverse design and optimization techniques for the multiobjective, multipoint design of turbomachinery blades. *Journal of Turbomachinery*, 131(2):021014.
<https://doi.org/10.1115/1.2950065>
- Bordoloi DJ, Tiwari R, 2017. Identification of suction flow blockages and casing cavitations in centrifugal pumps by optimal support vector machine techniques. *Journal of the Brazilian Society of Mechanical Sciences and Engineering*, 39(8):2957-2968.
<https://doi.org/10.1007/s40430-017-0714-z>
- Bowade A, Parashar C, 2015. A review of different blade design methods for radial flow centrifugal pump. *International Journal of Scientific Engineering and Research*, 3(7):24-27.
- Brennen EC, 2005. Fundamentals of Multiphase Flow. Cambridge University Press, New York, USA.
<https://doi.org/10.1017/CBO9780511807169>
- Bykov RK, Jacobsen CB, Pedersen N, 2003. Flow in a centrifugal pump impeller at design and off-design conditions—part II: large eddy simulations. *Journal of Fluids Engineering*, 125(1):73-83.
<https://doi.org/10.1115/1.1524586>
- Caridad J, Asuaje M, Kenyery F, et al., 2008. Characterization of a centrifugal pump impeller under two-phase flow conditions. *Journal of Petroleum Science and Engineering*, 63(1-4):18-22.
<https://doi.org/10.1016/j.petrol.2008.06.005>
- Cavazzini G, Pavesi G, Ardizzon G, 2011. Pressure instabilities in a vaned centrifugal pump. *Proceedings of the Institution of Mechanical Engineers, Part A: Journal of Power and Energy*, 225(7):930-939.
<https://doi.org/10.1177/0957650911410643>
- Cavazzini G, Pavesi G, Santolin A, et al., 2015. Using splitter blades to improve suction performance of centrifugal impeller pumps. *Proceedings of the Institution of Mechanical Engineers, Part A: Journal of Power and Energy*, 229(3):309-323.
<https://doi.org/10.1177/0957650914563364>
- Černetič J, 2009. The use of noise and vibration signals for detecting cavitation in kinetic pumps. *Proceedings of the Institution of Mechanical Engineers, Part C: Journal of Mechanical Engineering Science*, 223(7):1645-1655.
<https://doi.org/10.1243/09544062jmes1404>
- Chalghoum I, Elaoud S, Akrouf M, et al., 2016. Transient behavior of a centrifugal pump during starting period. *Applied Acoustics*, 109:82-89.
<https://doi.org/10.1016/j.apacoust.2016.02.007>
- Chalghoum I, Elaoud S, Kanfoudi H, et al., 2018. The effects of the rotor-stator interaction on unsteady pressure pulsation and radial force in a centrifugal pump. *Journal of Hydrodynamics*, 30(4):672-681.
<https://doi.org/10.1007/s42241-018-0073-y>
- Chang H, Shi WD, Li W, et al., 2020. Experimental optimization of jet self-priming centrifugal pump based on orthogonal design and grey-correlational method. *Journal of Thermal Science*, 29:241-250.
<https://doi.org/10.1007/s11630-019-1160-2>
- Chen HX, Ma Z, Zhang W, et al., 2017a. On the hydrodynamics of hydraulic machinery and flow control. *Journal of Hydrodynamics*, 29(5):782-789.
[https://doi.org/10.1016/S1001-6058\(16\)60789-8](https://doi.org/10.1016/S1001-6058(16)60789-8)
- Chen HX, He JW, Liu C, 2017b. Design and experiment of the centrifugal pump impellers with twisted inlet vice blades. *Journal of Hydrodynamics*, 29(6):1085-1088.
[https://doi.org/10.1016/S1001-6058\(16\)60822-3](https://doi.org/10.1016/S1001-6058(16)60822-3)
- Cheng ZW, Tong SG, Tong ZM, 2019. Bi-directional nozzle control of multistage radial-inflow turbine for optimal part-load operation of compressed air energy storage. *Energy Conversion and Management*, 181:485-500.
<https://doi.org/10.1016/j.enconman.2018.12.014>
- Choi JS, McLaughlin DK, Thompson DE, 2003. Experiments on the unsteady flow field and noise generation in a centrifugal pump impeller. *Journal of Sound and Vibration*, 263(3):493-514.
[https://doi.org/10.1016/S0022-460X\(02\)01061-1](https://doi.org/10.1016/S0022-460X(02)01061-1)
- Chudina M, 2003. Noise as an indicator of cavitation in a centrifugal pump. *Acoustical Physics*, 49(4):463-474.
<https://doi.org/10.1134/1.1591303>
- Čudina M, Prezelj J, 2009. Detection of cavitation in operation of kinetic pumps. Use of discrete frequency tone in audible spectra. *Applied Acoustics*, 70(4):540-546.
<https://doi.org/10.1016/j.apacoust.2008.07.005>
- Deb K, Jain H, 2014. An evolutionary many-objective optimization algorithm using reference-point-based non-dominated sorting approach, part I: solving problems with box constraints. *IEEE Transactions on Evolutionary Computation*, 18(4):577-601.

- <https://doi.org/10.1109/Tevc.2013.2281535>
- de Giorgi MG, Ficarella A, Lay-Ekuakille A, 2015. Monitoring cavitation regime from pressure and optical sensors: comparing methods using wavelet decomposition for signal processing. *IEEE Sensors Journal*, 15(8):4684-4691.
<https://doi.org/10.1109/JSEN.2015.2427369>
- Derakhshan S, Bashiri M, 2018. Investigation of an efficient shape optimization procedure for centrifugal pump impeller using eagle strategy algorithm and ANN (case study: slurry flow). *Structural and Multidisciplinary Optimization*, 58(2):459-473.
<https://doi.org/10.1007/s00158-018-1897-3>
- Derakhshan S, Pourmahdavi M, Abdolahnejad E, et al., 2013. Numerical shape optimization of a centrifugal pump impeller using artificial bee colony algorithm. *Computers & Fluids*, 81:145-151.
<https://doi.org/10.1016/j.compfluid.2013.04.018>
- Ding H, Visser FC, Jiang Y, et al., 2011. Demonstration and validation of a 3D CFD simulation tool predicting pump performance and cavitation for industrial applications. *Journal of Fluids Engineering*, 133(1):011101.
<https://doi.org/10.1115/1.4003196>
- Dong L, Zhao YQ, Dai C, 2019. Detection of inception cavitation in centrifugal pump by fluid-borne noise diagnostic. *Shock and Vibration*, 2019:9641478.
<https://doi.org/10.1155/2019/9641478>
- Dou HS, Jiang W, 2013. Application of energy gradient theory in flow instability in a centrifugal pump. *IOP Conference Series: Materials Science and Engineering*, 52(1):012007.
<https://doi.org/10.1088/1757-899x/52/1/012007>
- Fang HB, Wang Q, Tu YC, et al., 2008. An efficient non-dominated sorting method for evolutionary algorithms. *Evolutionary Computation*, 16(3):355-384.
<https://doi.org/10.1162/evco.2008.16.3.355>
- Farokhzad S, Bakhtyari N, Ahmadi H, 2013. Vibration signals analysis and condition monitoring of centrifugal pump. *Technical Journal of Engineering and Applied Sciences*, 3(12):1081-1085.
- Feng J, Benra FK, Dohmen HJ, 2007. Qualitative comparison between numerical and experimental results of unsteady flow in a radial diffuser pump. *Journal of Visualization*, 10(4):349-357.
<https://doi.org/10.1007/bf03181893>
- Feng J, Benra FK, Dohmen HJ, 2009. Unsteady flow visualization at part-load conditions of a radial diffuser pump: by PIV and CFD. *Journal of Visualization*, 12(1):65-72.
<https://doi.org/10.1007/bf03181944>
- Feng J, Benra FK, Dohmen HJ, 2011. Investigation of periodically unsteady flow in a radial pump by CFD simulations and LDV measurements. *Journal of Turbomachinery*, 133(1):011004.
<https://doi.org/10.1115/1.4000486>
- Fu YX, Yuan JP, Yuan SQ, et al., 2015. Numerical and experimental analysis of flow phenomena in a centrifugal pump operating under low flow rates. *Journal of Fluids Engineering*, 137(1):011102.
<https://doi.org/10.1115/1.4027142>
- Gaetani P, Boccazzi A, Sala R, 2012. Low field in the vaned diffuser of a centrifugal pump at different vane setting angles. *Journal of Fluids Engineering*, 134(3):031101.
<https://doi.org/10.1115/1.4005902>
- Gao B, Zhang N, Li Z, et al., 2016. Influence of the blade trailing edge profile on the performance and unsteady pressure pulsations in a low specific speed centrifugal pump. *Journal of Fluids Engineering*, 138(5):051106.
<https://doi.org/10.1115/1.4031911>
- Gao B, Guo PM, Zhang N, et al., 2017. Experimental investigation on cavitating flow induced vibration characteristics of a low specific speed centrifugal pump. *Shock and Vibration*, 2017:6568930.
<https://doi.org/10.1155/2017/6568930>
- Goel T, Dorney DJ, Haftka RT, et al., 2008. Improving the hydrodynamic performance of diffuser vanes via shape optimization. *Computers & Fluids*, 37(6):705-723.
<https://doi.org/10.1016/j.compfluid.2007.10.002>
- Golbabaei Asl M, Torabi R, Nourbakhsh SA, 2009. Experimental and FEM failure analysis and optimization of a centrifugal-pump volute casing. *Engineering Failure Analysis*, 16(6):1996-2003.
<https://doi.org/10.1016/j.engfailanal.2009.02.006>
- Goyal D, Pabla BS, 2016. The vibration monitoring methods and signal processing techniques for structural health monitoring: a review. *Archives of Computational Methods in Engineering*, 23(4):585-594.
<https://doi.org/10.1007/s11831-015-9145-0>
- Guleren KM, 2018. Automatic optimization of a centrifugal pump based on impeller-diffuser interaction. *Proceedings of the Institution of Mechanical Engineers, Part A: Journal of Power and Energy*, 232(8):1004-1018.
<https://doi.org/10.1177/0957650918766688>
- Guleren KM, Pinarbasi A, 2004. Numerical simulation of the stalled flow within a vaned centrifugal pump. *Proceedings of the Institution of Mechanical Engineers, Part C: Journal of Mechanical Engineering Science*, 218(4):425-435.
<https://doi.org/10.1177/095440620421800407>
- Guo R, Li RN, Zhang RH, 2019. Reconstruction and prediction of flow field fluctuation intensity and flow-induced noise in impeller domain of jet centrifugal pump using gappy pod method. *Energies*, 12(1):111.
<https://doi.org/10.3390/en12010111>
- Guo XM, Zhu ZC, Cui BL, et al., 2016. Effects of the number of inducer blades on the anti-cavitation characteristics and external performance of a centrifugal pump. *Journal of Mechanical Science and Technology*, 30(7):3173-3181.
<https://doi.org/10.1007/s12206-016-0510-1>
- Heo MW, Ma SB, Shim HS, et al., 2016. High-efficiency design optimization of a centrifugal pump. *Journal of*

- Mechanical Science and Technology*, 30(9):3917-3927.
<https://doi.org/10.1007/s12206-016-0803-4>
- Hergt PH, 1999. Pump research and development: past, present, and future. *Journal of Fluids Engineering*, 121(2): 248-253.
<https://doi.org/10.1115/1.2822198>
- Hirschi R, Dupont P, Avellan F, et al., 1998. Centrifugal pump performance drop due to leading edge cavitation: numerical predictions compared with model tests. *Journal of Fluids Engineering*, 120(4):705-711.
<https://doi.org/10.1115/1.2820727>
- Hu JK, Tong ZM, Xin JG, et al., 2019. Correspondence: simulation and experiment of a remotely operated underwater vehicle with cavitation jet technology. *Journal of Zhejiang University-SCIENCE A (Applied Physics & Engineering)*, 20(10):804-810.
<https://doi.org/10.1631/jzus.A1900356>
- Huang RF, Luo XW, Ji B, et al., 2015. Multi-objective optimization of a mixed-flow pump impeller using modified NSGA-II algorithm. *Science China Technological Sciences*, 58(12):2122-2130.
<https://doi.org/10.1007/s11431-015-5865-5>
- Huang YL, 2019. Research on Flow Field and Pressure Pulsation Characteristics of Centrifugal Pump Based on Laser Diagnosis Technology. MS Thesis, Harbin Engineering University, Harbin, China (in Chinese).
- Jafarzadeh B, Hajari A, Alishahi MM, et al., 2011. The flow simulation of a low-specific-speed high-speed centrifugal pump. *Applied Mathematical Modelling*, 35(1):242-249.
<https://doi.org/10.1016/j.apm.2010.05.021>
- Jiang QF, Heng YG, Liu XB, et al., 2019. A review of design considerations of centrifugal pump capability for handling inlet gas-liquid two-phase flows. *Energies*, 12(6): 1078.
<https://doi.org/10.3390/en12061078>
- Jiang W, 2015. Study on Mechanism of Flow Instability and Improvement of Centrifugal Pump. MS Thesis, Zhejiang Sci-Tech University, Hangzhou, China (in Chinese).
- Jin R, Chen W, Simpson TW, 2001. Comparative studies of metamodelling techniques under multiple modelling criteria. *Structural and Multidisciplinary Optimization*, 23(1):1-13.
<https://doi.org/10.1007/s00158-001-0160-4>
- Kadambi JR, Charoenngam P, Subramanian A, et al., 2004. Investigations of particle velocities in a slurry pump using PIV: part 1, the tongue and adjacent channel flow. *Journal of Energy Resources Technology*, 126(4):271-278.
<https://doi.org/10.1115/1.1786928>
- Kaewnai S, Chamaoot M, Wongwises S, 2009. Predicting performance of radial flow type impeller of centrifugal pump using CFD. *Journal of Mechanical Science and Technology*, 23(6):1620-1627.
<https://doi.org/10.1007/s12206-008-1106-1>
- Keller J, Blanco E, Barrio R, et al., 2014. PIV measurements of the unsteady flow structures in a volute centrifugal pump at a high flow rate. *Experiments in Fluids*, 55(10):1820.
<https://doi.org/10.1007/s00348-014-1820-7>
- Kim JH, Oh KT, Pyun KB, et al., 2013. Design optimization of a centrifugal pump impeller and volute using computational fluid dynamics. *IOP Conference Series: Earth and Environmental Science*, 15:032025.
<https://doi.org/10.1088/1755-1315/15/3/032025>
- Kim JH, Lee HC, Kim JH, et al., 2015. Design techniques to improve the performance of a centrifugal pump using CFD. *Journal of Mechanical Science and Technology*, 29(1):215-225.
<https://doi.org/10.1007/s12206-014-1228-6>
- Li WG, 2008. Numerical study on behavior of a centrifugal pump when delivering viscous oils—part 2: internal flow. *International Journal of Turbo & Jet-Engines*, 25(2):81-94.
<https://doi.org/10.1515/TJJ.2008.25.2.81>
- Li XJ, Yuan SQ, Pan ZY, et al., 2013. Numerical simulation of leading edge cavitation within the whole flow passage of a centrifugal pump. *Science China Technological Sciences*, 56(9):2156-2162.
<https://doi.org/10.1007/s11431-013-5311-5>
- Li XJ, Gao PL, Zhu ZC, et al., 2018. Effect of the blade loading distribution on hydrodynamic performance of a centrifugal pump with cylindrical blades. *Journal of Mechanical Science and Technology*, 32(3):1161-1170.
<https://doi.org/10.1007/s12206-018-0219-4>
- Li Y, Feng GQ, Li XJ, et al., 2018. An experimental study on the cavitation vibration characteristics of a centrifugal pump at normal flow rate. *Journal of Mechanical Science and Technology*, 32(10):4711-4720.
<https://doi.org/10.1007/s12206-018-0918-x>
- Li ZF, Wu DZ, Wang LQ, et al., 2010. Numerical simulation of the transient flow in a centrifugal pump during starting period. *Journal of Fluids Engineering*, 132(8):081102.
<https://doi.org/10.1115/1.4002056>
- Li ZF, Wu P, Wu DZ, et al., 2011. Experimental and numerical study of transient flow in a centrifugal pump during startup. *Journal of Mechanical Science and Technology*, 25(3):749-757.
<https://doi.org/10.1007/s12206-011-0107-7>
- Lin Z, Xue W, 2018. Safety integrity level evaluation of nuclear centrifugal pump based on performance degradation data. *Advances in Mechanical Engineering*, 10(4):1-13.
<https://doi.org/10.1177/1687814018772389>
- Liu DM, Liu SH, Wu YL, et al., 2009. LES numerical simulation of cavitation bubble shedding on ALE 25 and ALE 15 hydrofoils. *Journal of Hydrodynamics*, 21(6):807-813.
[https://doi.org/10.1016/S1001-6058\(08\)60216-4](https://doi.org/10.1016/S1001-6058(08)60216-4)
- Liu HL, Wang Y, Yuan SQ, et al., 2010. Effects of blade number on characteristics of centrifugal pumps. *Chinese Journal of Mechanical Engineering*, 23(6):742-747.
<https://doi.org/10.3901/CJME.2010.06.742>
- Liu HL, Wang Y, Liu DX, et al., 2013a. Assessment of a turbulence model for numerical predictions of

- sheet-cavitating flows in centrifugal pumps? *Journal of Mechanical Science and Technology*, 27(9):2743-2750.
<https://doi.org/10.1007/s12206-013-0720-8>
- Liu HL, Liu DX, Wang Y, et al., 2013b. Experimental investigation and numerical analysis of unsteady attached sheetcavitating flows in a centrifugal pump. *Journal of Hydrodynamics*, 25(3):370-378.
[https://doi.org/10.1016/s1001-6058\(11\)60375-3](https://doi.org/10.1016/s1001-6058(11)60375-3)
- Liu HL, Wang K, Kim HB, et al., 2013c. Experimental investigation of the unsteady flow in a double-blade centrifugal pump impeller. *Science China Technological Sciences*, 56(4):812-817.
<https://doi.org/10.1007/s11431-013-5154-0>
- Liu M, Tan L, Cao SL, 2018. Design method of controllable blade angle and orthogonal optimization of pressure rise for a multiphase pump. *Energies*, 11(5):1048.
<https://doi.org/10.3390/en11051048>
- Liu XM, Zhang WB, 2010. Two schemes of multi-objective aerodynamic optimization for centrifugal impeller using response surface model and genetic algorithm. Proceedings of ASME Turbo Expo 2010: Power for Land, Sea, and Air, p.1041-1053.
- Liu XW, Li HC, Shi XX, et al., 2019. Application of bi-harmonic equation in impeller profile optimization design of an aero-centrifugal pump. *Engineering Computations*, 36(5):1764-1795.
<https://doi.org/10.1108/ec-08-2018-0378>
- Lu JX, Yuan SQ, Siva P, et al., 2017a. The characteristics investigation under the unsteady cavitation condition in a centrifugal pump. *Journal of Mechanical Science and Technology*, 31(3):1213-1222.
<https://doi.org/10.1007/s12206-017-0220-3>
- Lu JX, Yuan SQ, Parameswaran S, et al., 2017b. Investigation on the vibration and flow instabilities induced by cavitation in a centrifugal pump. *Advances in Mechanical Engineering*, 9(4):1-11.
<https://doi.org/10.1177/1687814017696225>
- Lu JX, Liu XB, Zeng YZ, et al., 2019. Detection of the flow state for a centrifugal pump based on vibration. *Energies*, 12(16):3066.
<https://doi.org/10.3390/en12163066>
- Lu NX, Bensow RE, Bark G, 2010. LES of unsteady cavitation on the delft twisted foil. *Journal of Hydrodynamics*, 22(S1):742-749.
[https://doi.org/10.1016/S1001-6058\(10\)60031-5](https://doi.org/10.1016/S1001-6058(10)60031-5)
- Luo KK, Wang Y, Liu HL, et al., 2019. Effect of suction chamber baffles on pressure fluctuations in a low specific speed centrifugal pump. *Journal of Vibroengineering*, 21(5):1441-1455.
<https://doi.org/10.21595/jve.2018.18943>
- Luo Y, Sun H, Yuan SQ, et al., 2015. Research on statistical characteristics of vibration in centrifugal pump. *Technical Journal of the Faculty of Engineering*, 38(1):49-61.
- Mandhare NA, Karunamurthy K, Ismail S, 2019. Compendious review on “internal flow physics and minimization of flow instabilities through design modifications in a centrifugal pump”. *Journal of Pressure Vessel Technology*, 141(5):051601.
<https://doi.org/10.1115/1.4043383>
- Mansour M, Wunderlich B, Thévenin D, 2018. Effect of tip clearance gap and inducer on the transport of two-phase air-water flows by centrifugal pumps. *Experimental Thermal and Fluid Science*, 99:487-509.
<https://doi.org/10.1016/j.expthermflusci.2018.08.018>
- Medvitz RB, Kunz RF, Boger DA, et al., 2002. Performance analysis of cavitating flow in centrifugal pumps using multiphase CFD. *Journal of Fluids Engineering*, 124(2):377-383.
<https://doi.org/10.1115/1.1457453>
- Meng L, He M, Zhou LJ, et al., 2016. Influence of impeller-tongue interaction on the unsteady cavitation behavior in a centrifugal pump. *Engineering Computations*, 33(1):171-183.
<https://doi.org/10.1108/ec-09-2014-0179>
- Miner SM, Beaudoin RJ, Flack RD, 1989. Laser velocimeter measurements in a centrifugal flow pump. *Journal of Turbomachinery*, 111(3):205-212.
<https://doi.org/10.1115/1.3262257>
- Monte Verde W, Biazussi JL, Sassim NA, et al., 2017. Experimental study of gas-liquid two-phase flow patterns within centrifugal pumps impellers. *Experimental Thermal and Fluid Science*, 85:37-51.
<https://doi.org/10.1016/j.expthermflusci.2017.02.019>
- Mousmoulis G, Karlsen-Davies N, Aggidis G, et al., 2019. Experimental analysis of cavitation in a centrifugal pump using acoustic emission, vibration measurements and flow visualization. *European Journal of Mechanics–B/Fluids*, 75:300-311.
<https://doi.org/10.1016/j.euromechflu.2018.10.015>
- Mouvanal S, Chatterjee D, Bakshi S, et al., 2018. Numerical prediction of potential cavitation erosion in fuel injectors. *International Journal of Multiphase Flow*, 104:113-124.
<https://doi.org/10.1016/j.ijmultiphaseflow.2018.03.005>
- Murakami M, Minemura K, 1974a. Effects of entrained air on the performance of a centrifugal pump: 1st report, performance and flow conditions. *Bulletin of JSME*, 17(110):1047-1055.
<https://doi.org/10.1299/jsme1958.17.1047>
- Murakami M, Minemura K, 1974b. Effects of entrained air on the performance of centrifugal pumps: 2nd report, effects of number of blades. *Bulletin of JSME*, 17(112):1286-1295.
<https://doi.org/10.1299/jsme1958.17.1286>
- Nataraj M, Arunachalam VP, 2006. Optimizing impeller geometry for performance enhancement of a centrifugal pump using the Taguchi quality concept. *Proceedings of the Institution of Mechanical Engineers, Part A: Journal of Power and Energy*, 220(7):765-782.
<https://doi.org/10.1243/09576509jpe184>
- Nourbakhsh A, Safikhani H, Derakhshan S, 2011. The comparison of multi-objective particle swarm optimization and NSGA II algorithm: applications in centrifugal

- pumps. *Engineering Optimization*, 43(10):1095-1113.
<https://doi.org/10.1080/0305215X.2010.542811>
- Panda AK, Rapur JS, Tiwari R, 2018. Prediction of flow blockages and impending cavitation in centrifugal pumps using support vector machine (SVM) algorithms based on vibration measurements. *Measurement*, 130:44-56.
<https://doi.org/10.1016/j.measurement.2018.07.092>
- Parrondo-Gayo JL, González-Pérez J, Fernández-Francos J, 2002. The effect of the operating point on the pressure fluctuations at the blade passage frequency in the volute of a centrifugal pump. *Journal of Fluids Engineering*, 124(3):784-790.
<https://doi.org/10.1115/1.1493814>
- Pavesi G, Cavazzini G, Ardizzone G, 2008. Time-frequency characterization of the unsteady phenomena in a centrifugal pump. *International Journal of Heat and Fluid Flow*, 29(5):1527-1540.
<https://doi.org/10.1016/j.ijheatfluidflow.2008.06.008>
- Pedersen N, Larsen PS, Jacobsen CB, 2003. Flow in a centrifugal pump impeller at design and off-design conditions —part I: particle image velocimetry (PIV) and laser Doppler velocimetry (LDV) measurements. *Journal of Fluids Engineering*, 125(1):61-72.
<https://doi.org/10.1115/1.1524585>
- Pei J, Yuan SQ, Yuan JP, 2013. Numerical analysis of periodic flow unsteadiness in a single-blade centrifugal pump. *Science China Technological Sciences*, 56(1):212-221.
<https://doi.org/10.1007/s11431-012-5044-x>
- Pei J, Wang WJ, Yuan SQ, 2016a. Multi-point optimization on meridional shape of a centrifugal pump impeller for performance improvement. *Journal of Mechanical Science and Technology*, 30(11):4949-4960.
<https://doi.org/10.1007/s12206-016-1015-7>
- Pei J, Wang WJ, Yuan SQ, et al., 2016b. Optimization on the impeller of a low-specific-speed centrifugal pump for hydraulic performance improvement. *Chinese Journal of Mechanical Engineering*, 29(5):992-1002.
<https://doi.org/10.3901/cjme.2016.0519.069>
- Pei J, Gan XC, Wang WJ, et al., 2019. Multi-objective shape optimization on the inlet pipe of a vertical inline pump. *Journal of Fluids Engineering*, 141(6):061108.
<https://doi.org/10.1115/1.4043056>
- Posa A, Lippolis A, Verzicco R, et al., 2011. Large-eddy simulations in mixed-flow pumps using an immersed-boundary method. *Computers & Fluids*, 47(1):33-43.
<https://doi.org/10.1016/j.compfluid.2011.02.004>
- Poullikkas A, 2003. Effects of two-phase liquid-gas flow on the performance of nuclear reactor cooling pumps. *Progress in Nuclear Energy*, 42(1):3-10.
[https://doi.org/10.1016/S0149-1970\(03\)80002-1](https://doi.org/10.1016/S0149-1970(03)80002-1)
- Rapur JS, Tiwari R, 2018. Automation of multi-fault diagnosing of centrifugal pumps using multi-class support vector machine with vibration and motor current signals in frequency domain. *Journal of the Brazilian Society of Mechanical Sciences and Engineering*, 40(6):278.
<https://doi.org/10.1007/s40430-018-1202-9>
- Safikhani H, Khalkhali A, Farajpoor M, 2011. Pareto based multi-objective optimization of centrifugal pumps using CFD, neural networks and genetic algorithms. *Engineering Applications of Computational Fluid Mechanics*, 5(1):37-48.
<https://doi.org/10.1080/19942060.2011.11015351>
- Sakthivel NR, Sugumaran V, Nair BB, 2010a. Comparison of decision tree-fuzzy and rough set-fuzzy methods for fault categorization of mono-block centrifugal pump. *Mechanical Systems and Signal Processing*, 24(6):1887-1906.
<https://doi.org/10.1016/j.ymssp.2010.01.008>
- Sakthivel NR, Sugumaran V, Babudevasenapati S, 2010b. Vibration based fault diagnosis of monoblock centrifugal pump using decision tree. *Expert Systems with Applications*, 37(6):4040-4049.
<https://doi.org/10.1016/j.eswa.2009.10.002>
- Sato S, Furukawa A, Takamatsu Y, 1996. Air-water two-phase flow performance of centrifugal pump impellers with various blade angles. *JSME International Journal Series B Fluids and Thermal Engineering*, 39(2):223-229.
<https://doi.org/10.1299/jsmeb.39.223>
- Schäfer T, Bieberle A, Neumann M, et al., 2015. Application of gamma-ray computed tomography for the analysis of gas holdup distributions in centrifugal pumps. *Flow Measurement and Instrumentation*, 46:262-267.
<https://doi.org/10.1016/j.flowmeasinst.2015.06.001>
- Scott SL, 2003. Multiphase pumping addresses a wide range of operating problems. *Oil & Gas Journal*, 101(37):59.
- Sekoguchi K, Takada S, Kanemori Y, 1984. Study of air-water two-phase centrifugal pump by means of electric resistivity probe technique for void fraction measurement: 1st report, measurement of void fraction distribution in a radial flow impeller. *Bulletin of JSME*, 27(227):931-938.
<https://doi.org/10.1299/jsme1958.27.931>
- Shah SR, Jain SV, Patel RN, et al., 2013. CFD for centrifugal pumps: a review of the state-of-the-art. *Procedia Engineering*, 51:715-720.
<https://doi.org/10.1016/j.proeng.2013.01.102>
- Shao CL, Zhou JF, Cheng WJ, 2015. Experimental and numerical study of external performance and internal flow of a molten salt pump that transports fluids with different viscosities. *International Journal of Heat and Mass Transfer*, 89:627-640.
<https://doi.org/10.1016/j.ijheatmasstransfer.2015.05.087>
- Shao CL, Li CQ, Zhou JF, 2018. Experimental investigation of flow patterns and external performance of a centrifugal pump that transports gas-liquid two-phase mixtures. *International Journal of Heat and Fluid Flow*, 71:460-469.
<https://doi.org/10.1016/j.ijheatfluidflow.2018.05.011>
- Shi WD, Zhou L, Lu WG, et al., 2013. Numerical prediction and performance experiment in a deep-well centrifugal pump with different impeller outlet width. *Chinese Journal of Mechanical Engineering*, 26(1):46-52.

- <https://doi.org/10.3901/cjme.2013.01.046>
- Shi WD, Wang C, Wang W, et al., 2014. Numerical calculation on cavitation pressure pulsation in centrifugal pump. *Advances in Mechanical Engineering*, 2014:367631. <https://doi.org/10.1155/2014/367631>
- Shim HS, Afzal A, Kim KY, et al., 2016. Three-objective optimization of a centrifugal pump with double volute to minimize radial thrust at off-design conditions. *Proceedings of the Institution of Mechanical Engineers, Part A: Journal of Power and Energy*, 230(6):598-615. <https://doi.org/10.1177/0957650916656544>
- Shim HS, Kim KY, Choi YS, 2018. Three-objective optimization of a centrifugal pump to reduce flow recirculation and cavitation. *Journal of Fluids Engineering*, 140(9):091202. <https://doi.org/10.1115/1.4039511>
- Shojaefard MH, Tahani M, Ehghaghi MB, et al., 2012. Corrigendum to “Numerical study of the effects of some geometric characteristics of a centrifugal pump impeller that pumps a viscous fluid” [Computers & Fluids 60 (2012) 61–70]. *Computers & Fluids*, 64:157. <https://doi.org/10.1016/j.compfluid.2012.06.014>
- Si QR, Yuan SQ, Yuan JP, et al., 2013. Multiobjective optimization of low-specific-speed multistage pumps by using matrix analysis and CFD method. *Journal of Applied Mathematics*, 2013:136195. <https://doi.org/10.1155/2013/136195>
- Si QR, Dupont P, Bayeul-Lainé AC, et al., 2015. An experimental study of the flow field inside the diffuser passage of a laboratory centrifugal pump. *Journal of Fluids Engineering*, 137(6):061105. <https://doi.org/10.1115/1.4029671>
- Si QR, Ali A, Yuan JP, et al., 2019. Flow-induced noises in a centrifugal pump: a review. *Science of Advanced Materials*, 11(7):909-924. <https://doi.org/10.1166/sam.2019.3617>
- Siddique MH, Afzal A, Samad A, 2018. Design optimization of the centrifugal pumps via low fidelity models. *Mathematical Problems in Engineering*, 2018:3987594. <https://doi.org/10.1155/2018/3987594>
- Singhal AK, Athavale MM, Li HY, et al., 2002. Mathematical basis and validation of the full cavitation model. *Journal of Fluids Engineering*, 124(3):617-624. <https://doi.org/10.1115/1.1486223>
- Song Y, Fan HG, Zhang W, et al., 2019. Flow characteristics in volute of a double-suction centrifugal pump with different impeller arrangements. *Energies*, 12(4):669. <https://doi.org/10.3390/en12040669>
- Stel H, Amaral GDL, Negrão COR, et al., 2013. Numerical analysis of the fluid flow in the first stage of a two-stage centrifugal pump with a vaned diffuser. *Journal of Fluids Engineering*, 135(7):071104. <https://doi.org/10.1115/1.4023956>
- Sun H, Yuan SQ, Luo Y, 2018. Cyclic spectral analysis of vibration signals for centrifugal pump fault characterization. *IEEE Sensors Journal*, 18(7):2925-2933. <https://doi.org/10.1109/jsen.2018.2804908>
- Tan L, Cao SL, Wang YM, et al., 2012. Numerical simulation of cavitation in a centrifugal pump at low flow rate. *Chinese Physics Letters*, 29(1):014702. <https://doi.org/10.1088/0256-307x/29/1/014702>
- Tan L, Zhu BS, Cao SL, et al., 2013. Cavitation flow simulation for a centrifugal pump at a low flow rate. *Chinese Science Bulletin*, 58(8):949-952. <https://doi.org/10.1007/s11434-013-5672-y>
- Tan L, Zhu BS, Cao SL, et al., 2014a. Influence of blade wrap angle on centrifugal pump performance by numerical and experimental study. *Chinese Journal of Mechanical Engineering*, 27(1):171-177. <https://doi.org/10.3901/cjme.2014.01.171>
- Tan L, Zhu BS, Cao SL, et al., 2014b. Influence of prewhirl regulation by inlet guide vanes on cavitation performance of a centrifugal pump. *Energies*, 7(2):1050-1065. <https://doi.org/10.3390/en7021050>
- Tan L, Zhu BS, Wang YC, et al., 2015. Numerical study on characteristics of unsteady flow in a centrifugal pump volute at partial load condition. *Engineering Computations*, 32(6):1549-1566. <https://doi.org/10.1108/Ec-05-2014-0109>
- Tang XL, Bian LY, Wang FJ, et al., 2013. Numerical investigations on cavitating flows with thermodynamic effects in a diffuser-type centrifugal pump. *Journal of Mechanical Science and Technology*, 27(6):1655-1664. <https://doi.org/10.1007/s12206-013-0413-3>
- Tao R, Xiao RF, Wang ZW, 2018a. Influence of blade leading-edge shape on cavitation in a centrifugal pump impeller. *Energies*, 11(10):2588. <https://doi.org/10.3390/en11102588>
- Tao R, Xiao RF, Zhu D, et al., 2018b. Multi-objective optimization of double suction centrifugal pump. *Proceedings of the Institution of Mechanical Engineers, Part C: Journal of Mechanical Engineering Science*, 232(6):1108-1117. <https://doi.org/10.1177/0954406217699020>
- Tong SG, Cheng ZW, Cong FY, et al., 2018. Developing a grid-connected power optimization strategy for the integration of wind power with low-temperature adiabatic compressed air energy storage. *Renewable Energy*, 125:73-86. <https://doi.org/10.1016/j.renene.2018.02.067>
- Tong SG, Zhao H, Liu HQ, et al., 2019. Optimization calculation method for efficiency of multistage split case centrifugal pump. *Journal of Zhejiang University (Engineering Science)*, 53(5):988-996 (in Chinese). <https://doi.org/10.3785/j.issn.1008-973X.2019.05.021>
- Tong ZM, Li Y, Westerdahl D, et al., 2019a. Exploring the effects of ventilation practices in mitigating in-vehicle exposure to traffic-related air pollutants in China. *Environment International*, 127:773-784. <https://doi.org/10.1016/j.envint.2019.03.023>

- Tong ZM, Chen Y, Tong SG, et al., 2019b. Multi-objective optimization design of low specific speed centrifugal pump based on NSGA-III algorithm. *China Mechanical Engineering*, in press (in Chinese).
- Tong ZM, Cheng ZW, Tong SG, 2019c. Preliminary design of multistage radial turbines based on rotor loss characteristics under variable operating conditions. *Energies*, 12(13): 2550.
<https://doi.org/10.3390/en12132550>
- van den Braembussche RA, 2008. Numerical optimization for advanced turbomachinery design. In: Thévenin D, Janiga G (Eds.), *Optimization and Computational Fluid Dynamics*. Springer, Berlin, Germany, p.147-189.
- Wang C, Shi WD, Wang XK, et al., 2017. Optimal design of multistage centrifugal pump based on the combined energy loss model and computational fluid dynamics. *Applied Energy*, 187:10-26.
<https://doi.org/10.1016/j.apenergy.2016.11.046>
- Wang GY, Senocak I, Shyy W, et al., 2001. Dynamics of attached turbulent cavitating flows. *Progress in Aerospace Sciences*, 37(6):551-581.
[https://doi.org/10.1016/S0376-0421\(01\)00014-8](https://doi.org/10.1016/S0376-0421(01)00014-8)
- Wang J, Wang Y, Liu HL, et al., 2015. An improved turbulence model for predicting unsteady cavitating flows in centrifugal pump. *International Journal of Numerical Methods for Heat & Fluid Flow*, 25(5):1198-1213.
<https://doi.org/10.1108/hff-07-2014-0205>
- Wang K, Liu HL, Zhou XH, et al., 2016. Experimental research on pressure fluctuation and vibration in a mixed flow pump. *Journal of Mechanical Science and Technology*, 30(1):179-184.
<https://doi.org/10.1007/s12206-015-1221-8>
- Wang K, Lu X, He XH, 2018. Experimental investigation of vibration characteristics in a centrifugal pump with vaned diffuser. *Shock and Vibration*, 2018:9486536.
<https://doi.org/10.1155/2018/9486536>
- Wang W, 2016. Research on Hydrodynamic Noise of Multistage Centrifugal Pump. MS Thesis, Jiangsu University, Nanjing, China (in Chinese).
- Wang WJ, Yuan SQ, Pei J, et al., 2017. Optimization of the diffuser in a centrifugal pump by combining response surface method with multi-island genetic algorithm. *Proceedings of the Institution of Mechanical Engineers, Part E: Journal of Process Mechanical Engineering*, 231(2):191-201.
<https://doi.org/10.1177/0954408915586310>
- Wang WJ, Osman MK, Pei J, et al., 2019. Artificial neural networks approach for a multi-objective cavitation optimization design in a double-suction centrifugal pump. *Processes*, 7(5):246.
<https://doi.org/10.3390/pr7050246>
- Wang XD, Hirsch C, Kang S, et al., 2011. Multi-objective optimization of turbomachinery using improved NSGA-II and approximation model. *Computer Methods in Applied Mechanics and Engineering*, 200(9-12):883-895.
<https://doi.org/10.1016/j.cma.2010.11.014>
- Wang Y, Liu HL, Liu DX, et al., 2016. Application of the two-phase three-component computational model to predict cavitating flow in a centrifugal pump and its validation. *Computers & Fluids*, 131:142-150.
<https://doi.org/10.1016/j.compfluid.2016.03.022>
- Wang YQ, Huo XW, 2018. Multiobjective optimization design and performance prediction of centrifugal pump based on orthogonal test. *Advances in Materials Science and Engineering*, 2018:6218178.
<https://doi.org/10.1155/2018/6218178>
- Wang YQ, Huo XW, Ji HL, 2018. Multiobjective optimization design and experimental study of desulfurization dust removal centrifugal pump based on immune particle swarm algorithm. *Advances in Materials Science and Engineering*, 2018:6294824.
<https://doi.org/10.1155/2018/6294824>
- Wei L, Wang C, Shi WD, et al., 2017. Numerical calculation and optimization designs in engine cooling water pump. *Journal of Mechanical Science and Technology*, 31(5): 2319-2329.
<https://doi.org/10.1007/s12206-017-0428-2>
- Westra RW, Broersma L, van Andel K, et al., 2010. PIV measurements and CFD computations of secondary flow in a centrifugal pump impeller. *Journal of Fluids Engineering*, 132(6):061104.
<https://doi.org/10.1115/1.4001803>
- Wood GM, Murphy JS, Farquhar J, 1960. An experimental study of cavitation in a mixed flow pump impeller. *Journal of Basic Engineering*, 82(4):929-940.
<https://doi.org/10.1115/1.3662806>
- Wu DZ, Wu P, Li ZF, et al., 2010. The transient flow in a centrifugal pump during the discharge valve rapid opening process. *Nuclear Engineering and Design*, 240(12): 4061-4068.
<https://doi.org/10.1016/j.nucengdes.2010.08.024>
- Wu KH, Lin BJ, Hung CI, 2008. Novel design of centrifugal pump impellers using generated machining method and CFD. *Engineering Applications of Computational Fluid Mechanics*, 2(2):195-207.
<https://doi.org/10.1080/19942060.2008.11015221>
- Wu YL, Liu SH, Yuan HJ, et al., 2011. PIV measurement on internal instantaneous flows of a centrifugal pump. *Science China Technological Sciences*, 54(2):270-276.
<https://doi.org/10.1007/s11431-010-4262-3>
- Xue R, Cai YJ, Fang XF, et al., 2019. Optimization study on a novel high-speed oil-free centrifugal water pump with hydrodynamic bearings. *Applied Sciences*, 9(15):3050.
<https://doi.org/10.3390/app9153050>
- Yang W, Xiao RF, 2014. Multiobjective optimization design of a pump-turbine impeller based on an inverse design using a combination optimization strategy. *Journal of Fluids Engineering*, 136(1):014501.
<https://doi.org/10.1115/1.4025454>
- Yang W, Xiao RF, Wang FJ, et al., 2014. Influence of splitter

- blades on the cavitation performance of a double suction centrifugal pump. *Advances in Mechanical Engineering*, 2014:963197.
<https://doi.org/10.1155/2014/963197>
- Yang ZJ, Wang FJ, Zhou PJ, 2012. Evaluation of subgrid-scale models in large-eddy simulations of turbulent flow in a centrifugal pump impeller. *Chinese Journal of Mechanical Engineering*, 25(5):911-918.
<https://doi.org/10.3901/cjme.2012.05.911>
- Yao ZF, Wang FJ, Qu LX, et al., 2011. Experimental investigation of time-frequency characteristics of pressure fluctuations in a double-suction centrifugal pump. *Journal of Fluids Engineering*, 133(10):101303.
<https://doi.org/10.1115/1.4004959>
- Yoshida Y, Eguchi M, Motomura T, et al., 2010. Rotordynamic forces acting on three-bladed inducer under supersynchronous/synchronous rotating cavitation. *Journal of Fluids Engineering*, 132(6):061105.
<https://doi.org/10.1115/1.3425727>
- Zargar OA, 2014. Detecting cavitation in a vertical sea water centrifugal lift pump related to Iran oil industry cooling water circulation system. *Universal Journal of Mechanical Engineering*, 2(4):125-131.
<https://doi.org/10.13189/ujme.2014.020401>
- Zhang JF, Appiah D, Zhang F, et al., 2019. Experimental and numerical investigations on pressure pulsation in a pump mode operation of a pump as turbine. *Energy Science & Engineering*, 7(4):1264-1279.
<https://doi.org/10.1002/ese3.344>
- Zhang JY, Zhu HW, Yang C, et al., 2011. Multi-objective shape optimization of helico-axial multiphase pump impeller based on NSGA-II and ANN. *Energy Conversion and Management*, 52(1):538-546.
<https://doi.org/10.1016/j.enconman.2010.07.029>
- Zhang JY, Cai SJ, Li YJ, et al., 2016. Visualization study of gas-liquid two-phase flow patterns inside a three-stage rotodynamic multiphase pump. *Experimental Thermal and Fluid Science*, 70:125-138.
<https://doi.org/10.1016/j.expthermflusci.2015.08.013>
- Zhang N, Yang MG, Gao B, et al., 2016. Investigation of rotor-stator interaction and flow unsteadiness in a low specific speed centrifugal pump. *Strojniški Vestnik—Journal of Mechanical Engineering*, 62(1):21-31.
<https://doi.org/10.5545/sv-jme.2015.2859>
- Zhang N, Gao B, Li Z, et al., 2018. Unsteady flow structure and its evolution in a low specific speed centrifugal pump measured by PIV. *Experimental Thermal and Fluid Science*, 97:133-144.
<https://doi.org/10.1016/j.expthermflusci.2018.04.013>
- Zhang QF, Li H, 2007. MOEA/D: a multiobjective evolutionary algorithm based on decomposition. *IEEE Transactions on Evolutionary Computation*, 11(6):712-731.
<https://doi.org/10.1109/TEVC.2007.892759>
- Zhang QH, Cao L, Yan ZX, et al., 2019. Hydraulics and blading of centrifugal pump impellers: a systematic review and application. *Iranian Journal of Science and Technology, Transactions of Mechanical Engineering*, 43(1):1-12.
<https://doi.org/10.1007/s40997-018-0203-8>
- Zhang RH, Guo R, Yang JH, et al., 2017. Inverse method of centrifugal pump impeller based on proper orthogonal decomposition (POD) method. *Chinese Journal of Mechanical Engineering*, 30(4):1025-1031.
<https://doi.org/10.1007/s10033-017-0137-x>
- Zhang Y, Wu JL, Zhang YQ, et al., 2014a. Design optimization of centrifugal pump using radial basis function metamodels. *Advances in Mechanical Engineering*, 2014:457542.
<https://doi.org/10.1155/2014/457542>
- Zhang Y, Hu SB, Wu JL, et al., 2014b. Multi-objective optimization of double suction centrifugal pump using Kriging metamodels. *Advances in Engineering Software*, 74:16-26.
<https://doi.org/10.1016/j.advengsoft.2014.04.001>
- Zhang Y, Hu SB, Zhang YQ, et al., 2014c. Optimization and analysis of centrifugal pump considering fluid-structure interaction. *The Scientific World Journal*, 2014:131802.
<https://doi.org/10.1155/2014/131802>
- Zhang YL, Zhu ZC, Li WG, 2016. Experiments on transient performance of a low specific speed centrifugal pump with open impeller. *Proceedings of the Institution of Mechanical Engineers, Part A: Journal of Power and Energy*, 230(7):648-659.
<https://doi.org/10.1177/0957650916666452>
- Zhao A, Lai ZN, Wu P, et al., 2016. Multi-objective optimization of a low specific speed centrifugal pump using an evolutionary algorithm. *Engineering Optimization*, 48(7):1251-1274.
<https://doi.org/10.1080/0305215x.2015.1104987>
- Zhao WG, Zhao GS, 2018. Numerical investigation on the transient characteristics of sediment-laden two-phase flow in a centrifugal pump. *Journal of Mechanical Science and Technology*, 32(1):167-176.
<https://doi.org/10.1007/s12206-017-1218-6>
- Zhao XR, Xiao YX, Wang ZW, et al., 2018. Unsteady flow and pressure pulsation characteristics analysis of rotating stall in centrifugal pumps under off-design conditions. *Journal of Fluids Engineering*, 140(2):021105.
<https://doi.org/10.1115/1.4037973>
- Zheng LL, Dou HS, Chen XP, et al., 2018. Pressure fluctuation generated by the interaction of blade and tongue. *Journal of Thermal Science*, 27(1):8-16.
<https://doi.org/10.1007/s11630-018-0978-3>
- Zhou L, Shi WD, Lu WG, et al., 2012. Numerical investigations and performance experiments of a deep-well centrifugal pump with different diffusers. *Journal of Fluids Engineering*, 134(7):071102.
<https://doi.org/10.1115/1.4006676>
- Zhou L, Shi WD, Wu SQ, 2013. Performance optimization in a centrifugal pump impeller by orthogonal experiment and

- numerical simulation. *Advances in Mechanical Engineering*, 2013:385809.
<https://doi.org/10.1155/2013/385809>
- Zhou L, Shi WD, Cao WD, et al., 2015. CFD investigation and PIV validation of flow field in a compact return diffuser under strong part-load conditions. *Science China Technological Sciences*, 58(3):405-414.
<https://doi.org/10.1007/s11431-014-5743-6>
- Zhou L, Shi WD, Li W, et al., 2016. Particle image velocimetry measurements and performance experiments in a compact return diffuser under different rotating speed. *Experimental Techniques*, 40(1):245-252.
<https://doi.org/10.1007/s40799-016-0028-6>
- Zhu JJ, Zhang HQ, 2018. A review of experiments and modeling of gas-liquid flow in electrical submersible pumps. *Energies*, 11(1):180.
<https://doi.org/10.3390/en11010180>
- Zhu YS, Zhu SS, Zhu DZ, et al., 2012. Predicting performance of centrifugal pump by combining genetic algorithm with BP neural network. *Mechanical Science and Technology*, 31(8):1274-1279 (in Chinese).
- Zouari R, Sieg-Zieba S, Sidahmed M, 2004. Fault detection system for centrifugal pumps using neural networks and neuro-fuzzy techniques. *Surveillance*, 5:11-13.

中文概要

题目: 离心泵内部流动结构、性能优化与故障检测综述

目的: 对离心泵的内部流动机理和外部特性、振动监测和性能优化进行研究, 并对新兴研究趋势进行评

述, 为提高离心泵系统的能效提供参考建议。

创新点: 1. 探讨了最新的用于离心泵数值模拟的湍流模型和空化模型的研究成果以及利用可视化方法揭示离心泵内部复杂流动现象的最新进展。2. 对离心泵的外部特性、空化和振动进行了广泛的讨论, 并总结出一种提高离心泵在工程应用中的效率和扬程、降低汽蚀余量的适用性强的离心泵叶轮多目标优化方法。

方法: 1. 对离心泵的内部流动机理进行综述, 以充分了解离心泵内部复杂的流场结构和能量损失机理。2. 对离心泵外部特性进行研究, 解释内部非定常流动与外部特性的耦合关系。3. 介绍与离心泵在运行过程中压力脉动的监测和测量相关的最新研究进展。4. 详细介绍优化离心泵性能的各种方法和措施。

结论: 1. 尽管对离心泵内部流动现象机理及流场结构的研究已经取得了一定进展, 但研究中仍存在一些亟待解决的问题, 如初生空化的监测与预防、泵内旋转失速现象发生发展的规律、数值模拟和实验之间不可忽视的数据差异等。2. 针对这些问题, 开发高精度的计算流体动力学仿真模型, 结合关键过流部件的优化设计来减少流动不稳定性和提高性能, 以及运用现代流动显示技术的最新设备进行大量的仔细繁杂的试验与测量工作, 是非常必要和重要的, 也是未来泵内流动研究的趋势。

关键词: 离心泵; 气液两相流; 空化机理; 压力脉动; 多目标优化